Australian Journal of Earth Sciences (2008) **55**, (1083–1106)

Cambrian paleosols and landscapes of South Australia*

G. J. RETALLACK

Department of Geological Sciences, University of Oregon, Eugene, OR 97403, USA (gregr@darkwing.uoregon.edu).

Cambrian marine, grey shales are widespread, and so are Cambrian intertidal, redbeds with weakly developed marine-influenced paleosols. A broader view of Cambrian landscapes and soilscapes now comes from paleosols of alluvial coastal plains of the Cambrian (to Ordovician?) Parachilna, Billy Creek, Moodlatana, Balcoracana, Pantapinna and Grindstone Range Formations in the central Flinders Ranges of South Australia. Paleosols are recognised by soil structures such as calcareous nodules (caliche) and cracked ridges (mukkara). They also show gradational changes down-profile in minerals, grainsize and chemical composition comparable with soils. Some of these Cambrian paleosols are thick (>1 m) and well developed (large caliche nodules). They indicate stable alluvial and coastal landscapes of quartzo-feldspathic and locally tuffaceous sediments. Paleoclimates were generally semiarid, although several intervals of subhumid paleoclimate coincide with local marine transgression. Drab-haloed filaments in red claystones, and elephant-skin and carpet textures in sandstones of some of the paleosols may be evidence of biological soil crusts, and some waterlogged marginal marine and lacustrine paleosols had animal burrows. Cambrian paleosols of the Flinders Ranges are assignable to the modern soil orders Vertisol, Aridisol, Inceptisol and Entisol. Modern soils of the Flinders Ranges and central Australia are within the same orders as the Cambrian paleosols, supporting evidence from paleogeomorphology that some Australian landscapes and soilscapes are very ancient indeed.

KEY WORDS: Cambrian, Flinders Ranges, paleosol, South Australia.

INTRODUCTION

Grey shales with trilobites characterise the Cambrian period where first established in Wales (*Cambria* of ancient Rome), as well as Cambrian marine rocks of Utah, British Columbia, eastern Siberia and Yunnan. Hints of Cambrian conditions on land come from supratidal red paleosols in the Georgina Basin of Queensland (Southgate 1986), the Cantabrian Mountains of Spain (Álvaro *et al*. 2003) and the Grand Canyon of Arizona (Rose 2006). My own field search on Cambrian rocks has discovered red intertidal paleosols near Cadiz, California (Waggoner & Hagadorn 2005), Waynesboro, Pennsylvania (Vetter *et al*. 1989), Beans Gap, Tennessee (Brooks 1955), Newport, Rhode Island (Skehan *et al*. 1987) and Caerfai Bay, Wales (Turner 1979). Without obviously terrestrial fossils such as dinosaurs and trees, Cambrian fully terrestrial environments have been difficult to recognise. Cambrian paleosols described here from South Australia now reveal differences between soils in intertidal and fluvial environments during this remote period of geological time. Also discovered with this work was evidence of biological activity in Cambrian paleosols. Surprisingly, Cambrian fluvial paleosols are not as different from modern soils as might be suspected for a geological time with such different terrestrial life.

Mawson & Segnit (1949) were first to propose non-marine paleoenvironments for Cambrian and Precambrian redbeds in the Flinders Ranges, based on their silty texture of highly angular grains like those of loess, and their strong oxidation in place. Briden (1967) noted Cambrian remnant magnetisation of hematite in the Billy Creek Formation in Balcoracana Creek. Cambrian soil formation in the Billy Creek to Grindstone Range Formations on Wirrealpa Station was argued by Stock (1974), who noted fluvial and intertidal facies with ferruginised clayey coatings, ferruginous replacement of feldspars, sharply alternating red and green beds, and red and green clasts redeposited in paleochannels. Moore (1990) also noted ferruginised biotite, oxide rims beneath as well as above silica coatings, and anomalous rarity of easily weathered pyroxene and amphibole. Reddened paleokarst was noted in the Wilkawillina Limestone and other shallow marine carbonates (Clarke 1990; Zang 2002), and one Early Cambrian paleokarst of regional extent was designated the 'Flinders Unconformity' (James & Gravestock 1990). Such criteria for recognition of Cambrian paleosols are further developed here, and the paleosols themselves are described,

*Appendix 1 [indicated by an asterisk (*) in the text and listed at the end of the paper] is a Supplementary Paper; copies may be obtained from the Geological Society of Australia's website (<http://www.gsa.org.au>) or from the National Library of Australia's Pandora archive (<http://nla.gov.au/nla.arc-25194>).

ISSN 0812-0099 print/ISSN 1440-0952 online
DOI: 10.1080/08120090802266568

categorised and analysed for clues to conditions on land at this remote period of geological history.

GEOLOGICAL SETTING

Cambrian rocks crop out on both flanks of the Blinman Dome, a diapiric breccia (Figure 1), on the eastern margin of the Arrowie Basin, a depositional basin between the Curnamona Craton to the east and the Gawler Craton to the west (Jago *et al.* 2002). Paleocurrents in the Moodlatana Formation, Pantapinna Sandstone and Grindstone Range Sandstone were to the north and east (Stock 1974), indicating source terranes in the Gawler Craton, rather than more distant eastern Curnamona Craton. During the Cambrian, South Australia was at about 20°N paleolatitude, continuous with China at about 40°N, on the northern margin of the Gondwana supercontinent (Jago *et al.* 2002).

The age of the Cambrian sequence in the central Flinders Ranges has been established by trilobites, chemostratigraphy and radiometry, with the following geological tie points in the reference section measured by Mawson (1939a) in Ten Mile Creek (Figure 2a). A marked negative carbon isotope ($\delta^{13}C_{carb.}$) excursion in the Woodendinna Dolomite, equivalent to 1152 m in Ten Mile Creek, has been correlated with the 538 Ma carbon isotope excursion of Siberia (Tucker 1991; Kirschvink & Raub 2003). A tuff in the basal Billy Creek Formation at 2389 m in Ten Mile Creek has yielded a $^{206}Pb/^{238}U$ SHRIMP zircon (SL13 standard) age of 522.8 ± 1.8 Ma (Haines & Flöttmann 1998; Gravestock & Shergold 2001). The first appearance of the trilobite *Redlichia guizhouensis* in the basal Wirrealpa Limestone at 3170 m in Ten Mile Creek has been correlated with the late Lungwangmaioan *R. guizhouensis* zone of China (Jago *et al.* 2002; Paterson & Brock 2007), which is dated at 511.5 Ma by Gradstein *et al.* (2004). Two other internationally correlatable trilobite occurrences are the first appearance of *Onaraspis rubra* in the Moodlatana Formation at 3533 m in Ten Mile Creek (Jago *et al.* 2002), taken as coeval with the 509.5 Ma *Oryctocephalus indicus* zone (Geyer & Shergold 2000; Gradstein *et al.* 2004), and the 504 Ma agnostid *Leiopyge laevigata* in the uppermost Balcoracana Formation in Lake Frome 3 (Daily & Forbes 1969), equivalent to at 3882 m in Ten Mile Creek.

Two of these tie points are controversial. The SHRIMP date has been revised for known problems with the SL13 standard, but is above Wilkawillina Limestone with the archaeocyathid *Syringocnema flavus* found in New South Wales below the Cymbric Vale tuff SHRIMP dated at 517.8 ± 2.1 Ma (Paterson 2005). Both dates are thus suspect, and also dubious is stratigraphic correlation using *Syringocnema flavus*. Identification of *Leiopyge laevigata* in the Balcoracana Formation in Lake Frome 3 was questioned by Jago *et al.* (2002, 2006), because it is uncertain whether this agnostid trilobite was originally or erosionally effaced, and the single specimen is now lost. Jago *et al.* (2002) also questioned whether Balcoracana Formation is present in that core, but my examination of the core revealed typical Balcoracana facies and paleosols (Irkili, Wandara and Warru pedotypes of Figure 2). Nevertheless, linear regression of these ages against stratigraphic levels is highly significant statistically

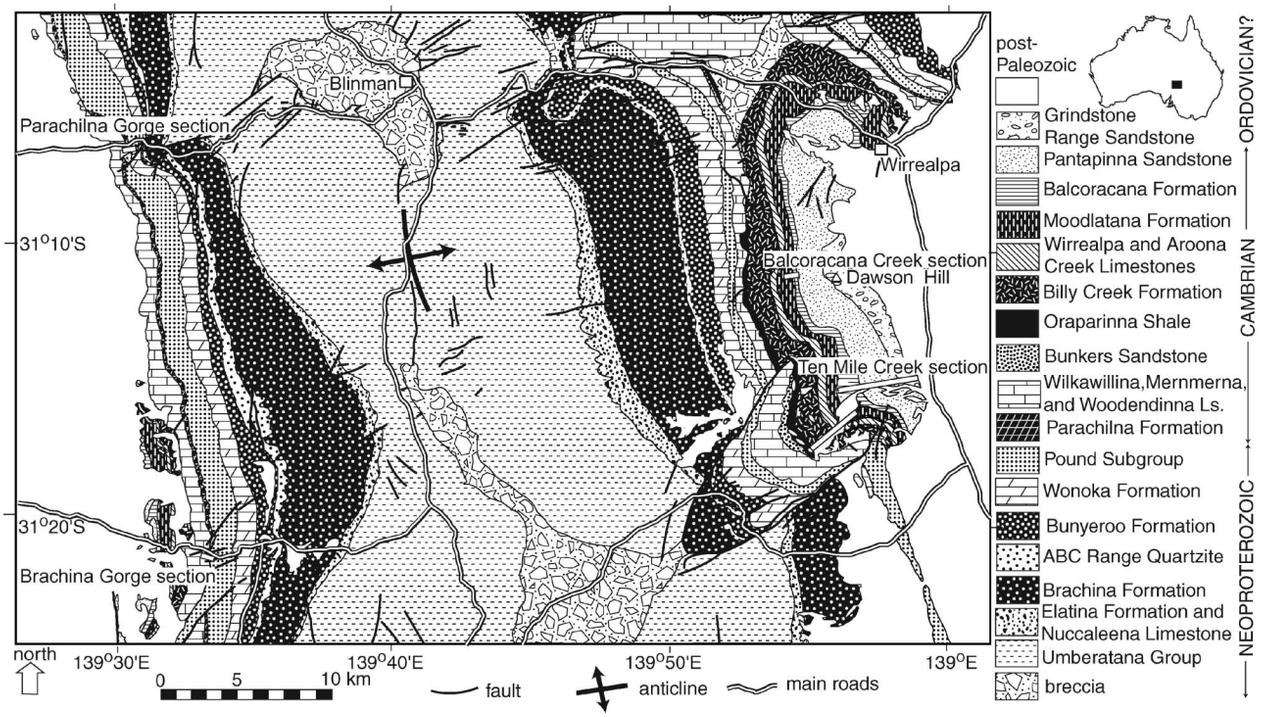

Figure 1 Geological map of Precambrian and Cambrian rocks of the Blinman Dome, eastern Arrowie Basin, Flinders Ranges, South Australia (modified from Dalgarno & Johnson 1966) showing sections examined for paleosols.

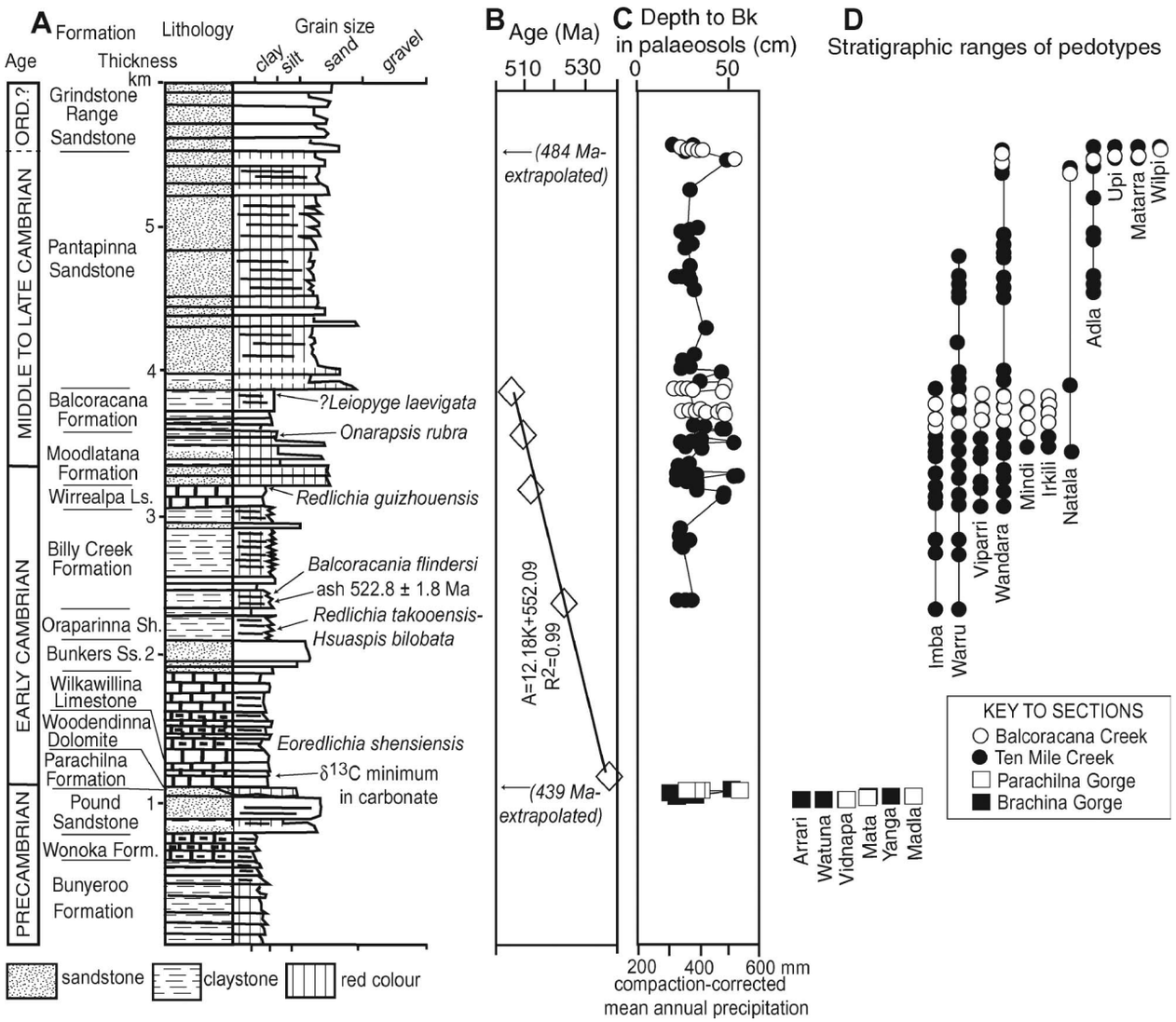

Figure 2 General geological section (a) along Ten Mile Creek, South Australia (based on Mawson 1939a), showing (b) stratigraphic tie points and linear interpolation formula (after Bengtson *et al.* 1990; Tucker 1991; Haines & Flöttmann 1998; Jago *et al.* 2002; Paterson & Brock 2007), (c) depth to calcareous nodules (Bk horizon of soil science) with paleosol profiles (above) as well as compaction corrected (using Sheldon & Retallack 2001) estimates of mean annual precipitation (following Retallack 2005) and (d) stratigraphic range of named pedotypes (Table 1).

(R^2 0.99: Figure 2b) with these controversial tie points, as well as without them.

Linear regression of the tie points (Figure 2b) can be used to extrapolate the age of the basal Woodendinna Dolomite (equivalent to 1052 m in Ten Mile Creek) as 539.1 Ma, younger than the Precambrian–Cambrian boundary at 542 Ma (Gradstein *et al.* 2004). This is expected, because conformably underlying the Woodendinna Dolomite in Parachilna and Brachina Gorges (but not Ten Mile Creek) is the Parachilna Formation (Dalgarno 1964), also of very early Cambrian age. The Parachilna Formation overlies basal Cambrian Uratanna Formation in the Mt Scott Range and Mudlapena Gap (Jensen *et al.* 1998), north of the study area (Figure 1). Either Parachilna or Uratanna Formation disconformably onlap paleotopography developed on the Ediacaran (latest Neoproterozoic) Rawnsley Quartzite due to coeval salt-tectonic uplift of the Blinman Dome (Gehling 2000).

Regression of ages against depth (Figure 2b) extrapolates to Early Ordovician ages of 478.2 Ma for the top of the sequence (6000 m in Ten Mile Creek), and a basal Ordovician age of 484.4 Ma for the base of the Grindstone Range Sandstone (at 5495 m). An Early Ordovician age of the Grindstone Range Sandstone was advocated by Daily (1976) and Moore (1990), but the Pantapinna and Grindstone Range Sandstones lack age diagnostic fossils and have subsequently been regarded as older than the Late Cambrian Delamerian Orogeny (Preiss 1995; Haines & Flöttmann 1998; Jago *et al.* 2002, 2006). Delamerian tectonism is now dated by many high-quality radiometric ages for granites, volcanic and metamorphic rocks, as well as fission-track unroofing-ages (Compston *et al.* 1966; Major & Teluk

1967; Milnes *et al*. 1977; Dalrymple 1979; Cooper *et al*. 1992; Zhou & Whitford 1994; Chen & Liu 1996; Turner 1996; Turner & Foden 1996; Turner *et al*. 1996; Haines & Flöttmann 1998; Mitchell *et al*. 1998, 2002; Foden *et al*. 1999, 2006; Burtt *et al*. 2000; Gibson & Stüwe 2000; Jenkins *et al*. 2002; Burtt & Phillips 2003; Elburg *et al*. 2003; Dutch *et al*. 2005). These radiometric dates show diachroneity from south to north (Figure 3). Linear regression of the geological age of granite cooling with present-day latitude shows that cooling migrated north at 10 mm/a, passing Brachina Gorge at 452.1 Ma, Ten Mile Creek at 451.2 Ma, Balcoracana Creek at 450.2 Ma, Parachilna Gorge 449.7 Ma: these ages are Late Ordovician (late Eastonian–Bolindian in Australian stages, or late Caradocian–Ashgillian in British Stages: Gradstein *et al*. 2004). Northward migration of Delamerian deformation is thus compatible with an Early Ordovician (Tremadocian) age of the Grindstone Range Sandstone (Figure 2b). If the very thick Pantapinna or Grindstone Range Sandstones were as old as Late Cambrian they should have evidence of exceptionally high sedimentation rates, as found in the late Early Cambrian White Point Conglomerate on Kangaroo Island, a synorogenic alluvial fan with boulders up to 50 cm diameter (Daily *et al*. 1980). Scattered vein quartz pebbles in the uppermost Grindstone Range Sandstone are well rounded and no more than 2 cm in diameter: comparable in size with pebbles and intraclasts in the Billy Creek Formation to Pantapinna Sandstone. An Early Ordovician age for the Grindstone Range Sandstone is plausible and unfalsified, but unproven.

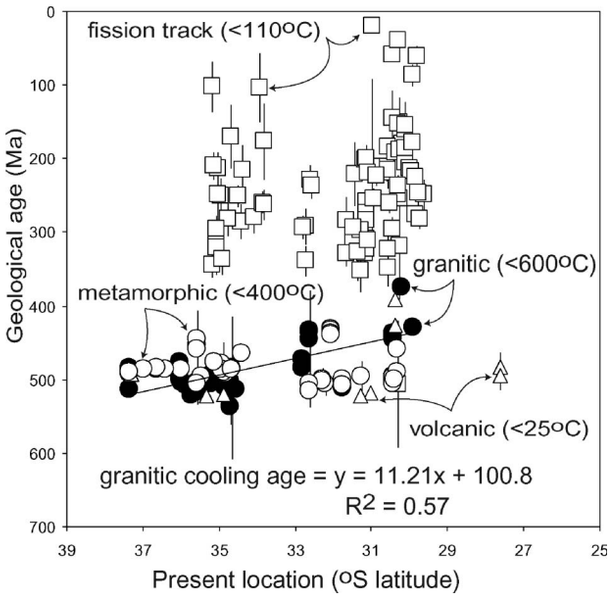

Figure 3 Regional diachroneity of Delamerian deformation and unroofing relevant to geological age of Grindstone Range Sandstone in the Arrowie Basin, from radiometric dating of volcanics (cooling through 25°C), granites (cooling through 600°C), metamorphic minerals (cooling through 400°C), and fission tracks (cooling through 110°C). Data are tabulated in Appendix 1*. Old K–Ar dates were corrected for new constants following Dalrymple (1979).

MATERIALS AND METHODS

Mawson's (1938, 1939a, b) classic sections on Ten Mile and Balcoracana Creeks, and Brachina and Parachilna Gorges (Figure 1) were reoccupied, noting subsequent stratigraphic and structural mapping by Dalgarno (1964), Dalgarno & Johnson (1966) and Clarke (1990). Thickness and size of soil features were recorded, as well as Munsell colour and reaction with dilute acid (Figure 2). Selected intervals were measured to record the position and nature of all paleosols (Figure 4). At least one representative profile of each recognisably different kind of paleosol (pedotype of Retallack 2001) was described in detail and sampled for laboratory studies of bulk chemical composition, thin-section petrography and mineral composition (Figures 5, 6). Locally named pedotypes bring order to the hundreds of paleosols logged, grouping them into 17 different kinds based on nominated type sections. Pedotypes are objective local field names, independent of modern soil classification and comparisons requiring laboratory analyses (Retallack 2001).

Petrographic thin-sections were used to quantify the grainsize (sand/silt/clay) and mineral composition of the paleosols, from 500 points on a Swift automated point counter and Leitz Orthoplan Pol research microscope. In addition, long axes of 1000 grains were measured using an ocular micrometer for granulometric analysis in the Krumbein phi scale [$\phi = -\log_2$ (mm)]. Bulk chemical analysis by XRF and FeO by potassium dichromate titration was done by ALS Chemex in Vancouver, Canada. Chemical and petrographic observations were supplemented with XRD traces from a Rigaku goniometer and microprobe mapping using a Cameca X100 with Noran System 6 Phase recognition software (Appendix 1*).

ALTERATION DUE TO BURIAL

The 5 km of Cambrian sediment observed in Ten Mile Creek (Figure 2) includes zircons with fission-track ages (Figure 3) indicating Late Paleozoic exhumation (temperatures <110°C), as well as post-mid-Cretaceous cooling (Mitchell *et al*. 1998, 2002). This is compatible with evidence from the Triassic, Leigh Creek Coal Measures, which are more than 610 m thick, and include sub-bituminous coals with specific energy of 25–29 kJ/g (Parkin 1969). Fluorescence colour and intensity of organic matter indicate increasing thermal alteration down the Cambrian section: equivalent to sub-bituminous–bituminous vitrinite reflectance of 0.5–1.53% in the Balcoracana Formation, 0.8–0.9% in the Moodlatana Formation, 1.11% in Wirrealpa Limestone and 1.16% in Oraparinna Shale (Zang 2002). Vitrinite reflectances are compatible with burial temperatures of about 100°C at the top of the sequence, and about 200°C in the Oraparinna Shale (Tissot & Welte 1984; Diessel 1992). Common volcanic shards and hyperdisplacive carbonate fabrics in paleosols of the lower Billy Creek Formation indicate a volcanic source, also confirmed by a dated ash (Haines & Flöttmann 1998). These sediments and paleosols may have once been amorphous colloids

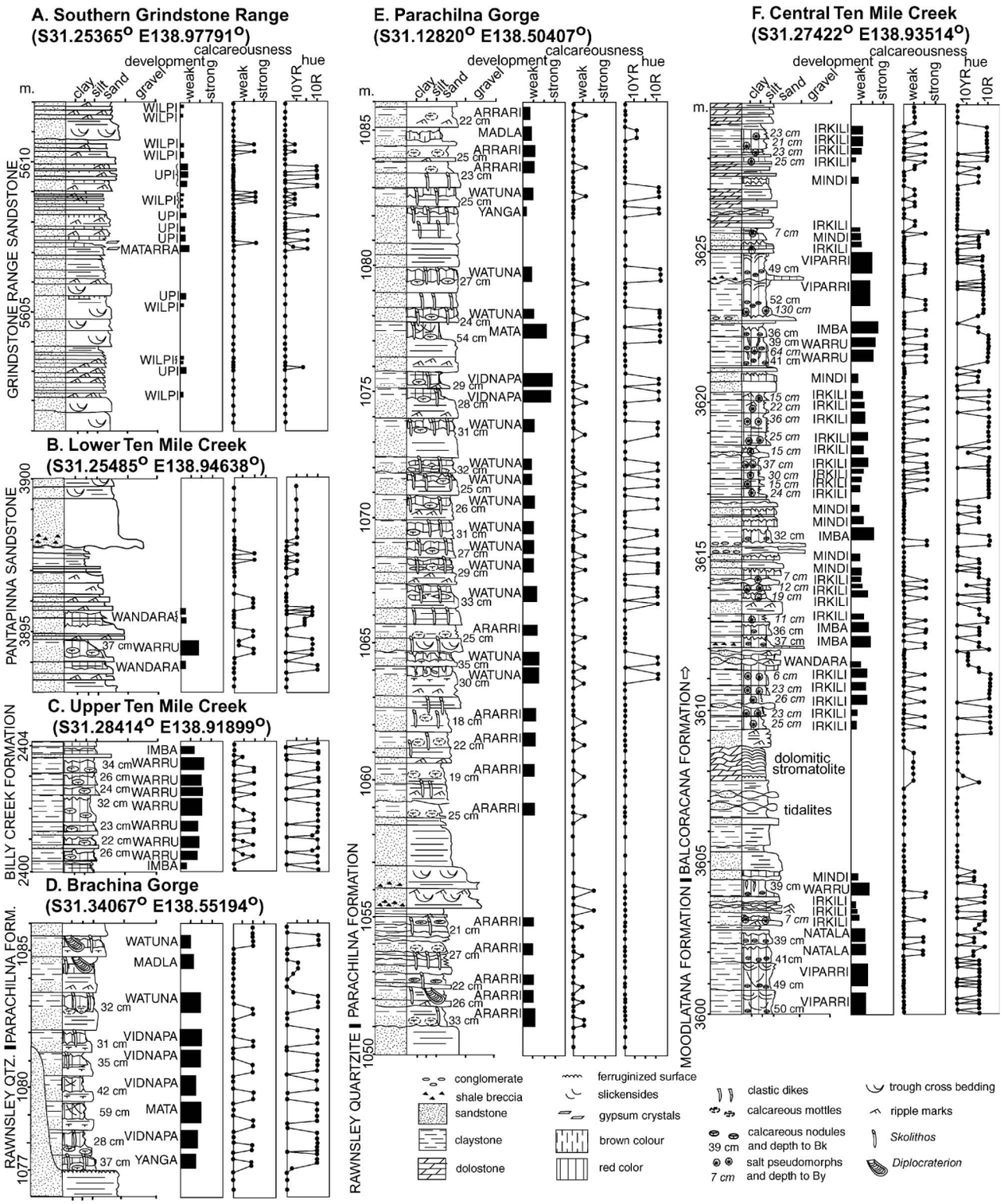

Figure 4 Measured sections of paleosols in the Cambrian Parachilna, Billy Creek, Moodlatana, Balcoracana, Pantapinna and Grindstone Range Formations of the Arrowie Basin, South Australia. Different pedotypes are named from the Adnamatna aboriginal language (McEntee & McKenzie 1992). Interpreted paleosols are indicated by height of black boxes, whose width represents relative degree of development as assessed in the field (Retallack 2001). Calcareousness assessed in field by degree of reaction with 10% stock HCl. Colours in column are weathered appearance, but numerical colours are from a Munsell chart. Metre levels are all relative to Ten Mile Creek section (Mawson 1939a).

(imogolite), now illitised, as in other volcaniclastic paleosols (Retallack 1991b; Retallack *et al.* 2000). Clay minerals in the Billy Creek to Balcoracana Formations include much authigenic illite and Mg and Fe chlorite, from alteration of original pedogenic smectites (Stock 1974), as is common during deep burial (Frey 1987;

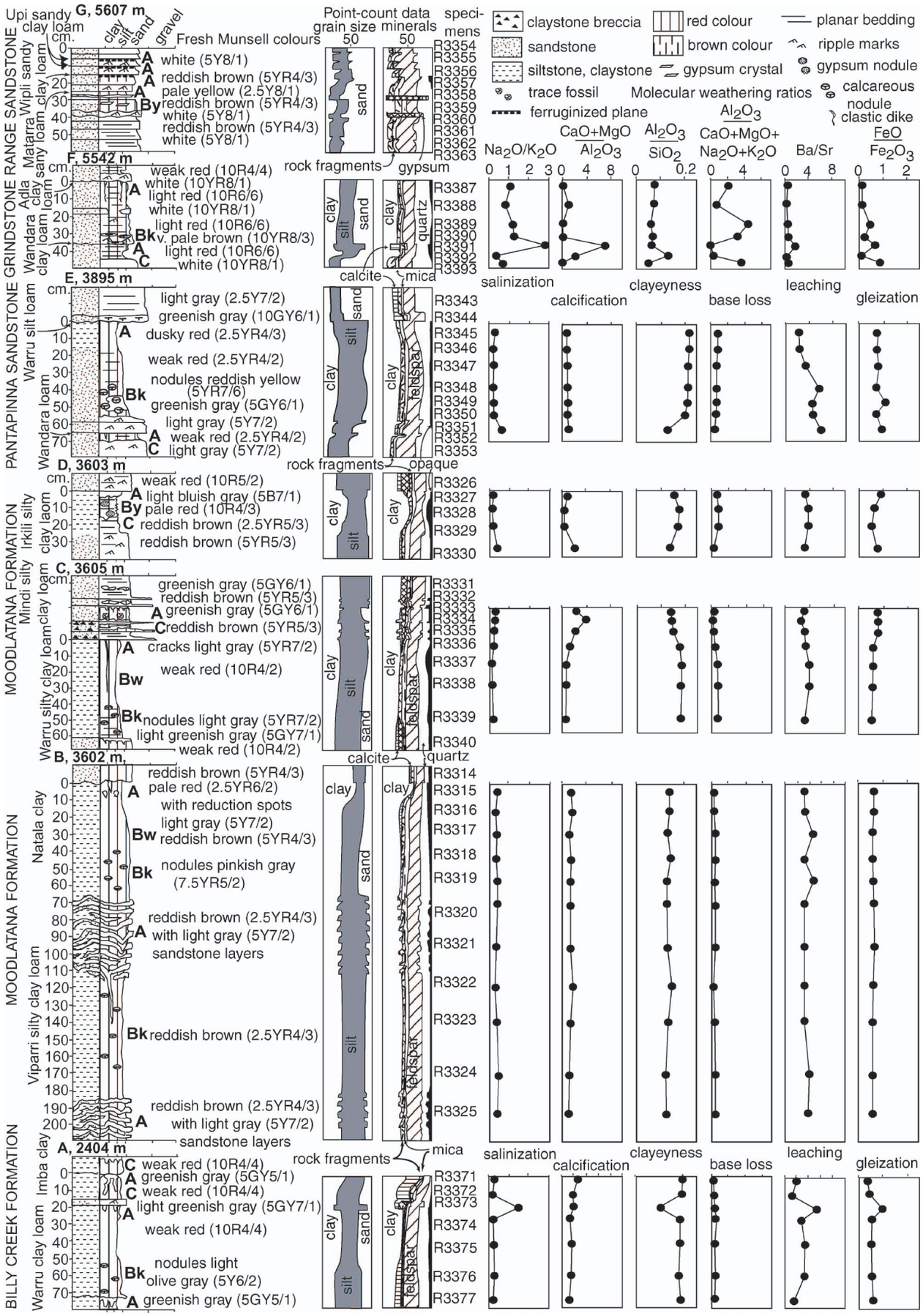
Upi sandy clay loam
G, 5607 m
clay silt sand gravel
Fresh Munsell colours
white (5Y8/1)
reddish brown (5YR4/3)
pale yellow (2.5Y8/1)
reddish brown (5YR4/3)
white (5Y8/1)
reddish brown (5YR4/3)
white (5Y8/1)
GRINDSTONE RANGE SANDSTONE
Wipli sandy clay loam
Matarra sany loam
F, 5542 m
weak red (10R4/4)
white (10YR8/1)
light red (10R6/6)
white (10YR8/1)
light red (10R6/6)
v. pale brown (10YR8/3)
light red (10R6/6)
white (10YR8/1)
Adla clay loam
Wandara clay loam
E, 3895 m
light gray (2.5Y7/2)
greenish gray (10GY6/1)
dusky red (2.5YR4/3)
weak red (2.5YR4/2)
nodules reddish yellow (5YR7/6)
greenish gray (5GY6/1)
light gray (5Y7/2)
weak red (2.5YR4/2)
light gray (5Y7/2)
PANTAPINNA SANDSTONE
Warru silt loam
Wandara loam
D, 3603 m
weak red (10R5/2)
light bluish gray (5B7/1)
pale red (10R4/3)
reddish brown (2.5YR5/3)
reddish brown (5YR5/3)
MOODLATANA FORMATION
Irkili silty clay laom
Mindi silty clay loam
C, 3605 m
greenish gray (5GY6/1)
reddish brown (5YR5/3)
greenish gray (5GY6/1)
reddish brown (5YR5/3)
cracks light gray (5YR7/2)
weak red (10R4/2)
nodules light gray (5YR7/2)
light greenish gray (5GY7/1)
weak red (10R4/2)
Warru silty clay loam
B, 3602 m,
reddish brown (5YR4/3)
pale red (2.5YR6/2)
with reduction spots
light gray (5Y7/2)
reddish brown (5YR4/3)
nodules pinkish gray (7.5YR5/2)
reddish brown (2.5YR4/3)
with light gray (5Y7/2)
sandstone layers
reddish brown (2.5YR4/3)
Natala clay
Viparri silty clay loam
reddish brown (2.5YR4/3)
with light gray (5Y7/2)
sandstone layers
BILLY CREEK FORMATION
Imba clay
Warru clay loam
A, 2404 m
weak red (10R4/4)
greenish gray (5GY5/1)
weak red (10R4/4)
light greenish gray (5GY7/1)
weak red (10R4/4)
nodules light olive gray (5Y6/2)
greenish gray (5GY5/1)
Point-count data
grain size
minerals
50
50
rock fragments
gypsum
calcite
mica
rock fragments
opaque
calcite
quartz
mica
clay
silt
sand
quartz
feldspar
specimens
R3354
R3355
R3356
R3357
R3358
R3359
R3360
R3361
R3362
R3363
R3387
R3388
R3389
R3390
R3391
R3392
R3393
R3343
R3344
R3345
R3346
R3347
R3348
R3349
R3350
R3351
R3352
R3353
R3326
R3327
R3328
R3329
R3330
R3331
R3332
R3333
R3334
R3335
R3336
R3337
R3338
R3339
R3340
R3314
R3315
R3316
R3317
R3318
R3319
R3320
R3321
R3322
R3323
R3324
R3325
R3371
R3372
R3373
R3374
R3375
R3376
R3377
claystone breccia
sandstone
siltstone, claystone
trace fossil
ferruginized plane
red colour
brown colour
gypsum crystal
Molecular weathering ratios
planar bedding
ripple marks
gypsum nodule
calcareous nodule
clastic dike
Na2O/K2O
CaO+MgO / Al2O3
Al2O3 / SiO2
CaO+MgO+ / Na2O+K2O
Ba/Sr
FeO / Fe2O3
0 1 2 3
0 4 8
0 0.2
0 4
0 4 8
0 1 2
salinization
calcification
clayeyness
base loss
leaching
gleization

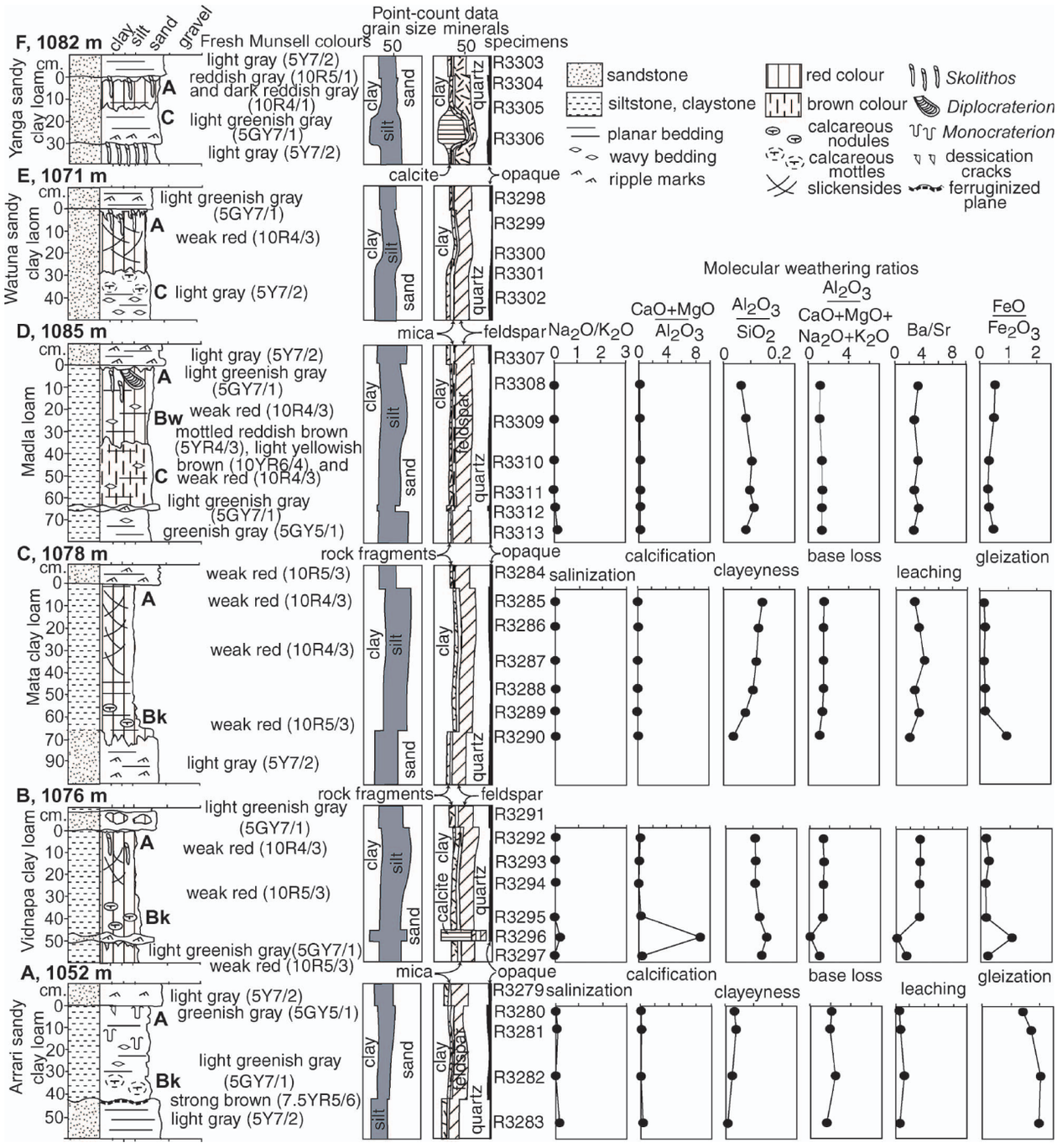

Figure 6 Field observations, interpreted soil horizons, grainsize and mineral content by point counting, and molecular weathering ratios from XRF chemical analysis of Lower Cambrian paleosols from the Parachilna Formation. Metre levels are all relative to the Ten Mile Creek section (Mawson 1939a).

Eberl *et al*. 1990). Weaver indices of illite crystallinity (10 Å/10.5 Å peak height) increase down-section (Figure 7), and exceed 2.3 in the lower part of the sequence, which was thus low in the greenschist facies of regional metamorphism (Frey 1987). Low-grade metamorphic alteration also is indicated by Kübler indices <0.42 and Weber indices less than 181 m below the Pantapinna Sandstone (Appendix 1*). Small amounts of pedogenic

Figure 5 Field observations, interpreted soil horizons, grainsize and mineral content by point counting, and molecular weathering ratios from XRF chemical analysis of Cambrian (–Ordovician?) paleosols from the Billy Creek, Moodlatana, Balcoracana, Pantapinna, and Grindstone Range Formations. Metre levels are all relative to the Ten Mile Creek section (Mawson 1939a).

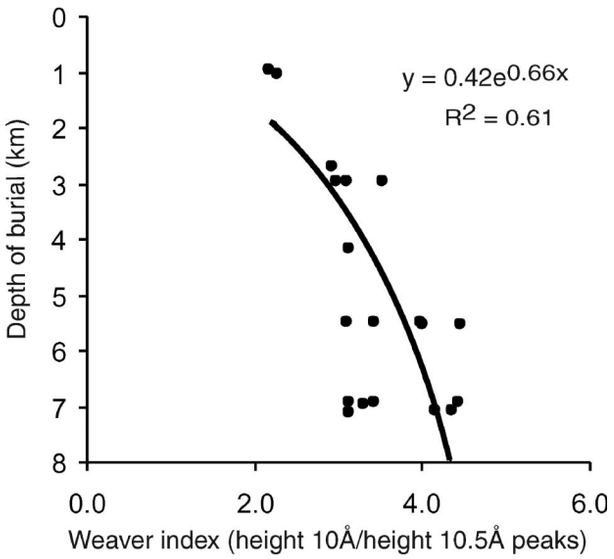

Figure 7 Weaver index (10 Å/10.5 Å peak height on X-ray diffractometer traces) *vs* depth of burial in Cambrian and Precambrian (>6.9 km burial) paleosols of the central Flinders Ranges.

smectite remain only in the Billy Creek Formation and higher units (Figure 8). Cambrian sequences of the central Flinders Ranges are thus highly altered diagenetically to weakly metamorphosed.

Other alterations of these Cambrian paleosols were created during very early burial. Clasts of redeposited red paleosol in grey-green paleochannel sandstones show green-grey rims from incomplete early burial gleisation (Figure 9c). Similarly, drab upper portions of most profiles may be due to burial gleisation of surficial organic matter by anaerobic microbes within overlying sediment consuming organic matter in the soil, as in geologically younger paleosols (Retallack 1991b, 2001). Marine rocks of the Mernmerna Formation, Oraparinna Shale and Wirrealpa Limestone have total organic carbon (TOC) of as much as 0.73–1.43%, but most Cambrian rocks of the Arrowie Basin have <0.4% TOC (Zang 2002). Early diagenetic organic matter decomposition may have deprived these paleosols and sediments of organic matter evident from body and trace fossils, as is usual for well-drained paleosols (Retallack 1991b). The red colour of the paleosols is likely due to hematite formed during early burial dehydration of iron oxyhydrates in originally orange and yellow soils (Retallack 1991b, 2001). Red colour could be due to reddening in Holocene or other post-Cambrian weathering, as in other Cambrian marine shales: the grey Emu Bay Shale beneath a coastal terrace soil of Kangaroo Island, South Australia (Daily *et al.* 1980), the grey Latham Shale near Cadiz, California (Waggoner & Hagadorn 2005), or the pyritic, black Yuanshan Shale of China in a Pleistocene lateritic profile at Maotianshan near Chengjiang (Chen 1994; Hu *et al.* 2004). Such post-Cambrian reddening is unlikely for the South Australian redbeds, because the Cambrian paleosols are not deeply weathered of bases (Figures 5, 6) and lack kaolinite (Figure 8) of South Australian Cretaceous to Cenozoic deep weathering (Firman 1994). Furthermore, Cambrian paleosols are the same colour and texture in outcrop and deep drillcore (to 782 m in Mt Frome 1–4), as noted also by Moore (1990).

PALEOSOL RECOGNITION

Cambrian marine rocks in the Flinders Ranges include black to grey shales, limestones and dolostones with trilobites, brachiopods, stromatolites, archaeocyathids, cyanobacterial sheaths and acritarchs (Pocock 1970; Jell 1983; Bengtson *et al.* 1990; Zang 2002; Jago *et al.* 2002; Paterson & Brock 2007). Also marine are sandstones and siltstones with trace fossils such *Cruziana*, *Skolithos*, *Diplocraterion* and *Monocraterion* (Jensen *et al.* 1998), although some marine trace fossils are in redbeds with halite hopper casts as evidence of exposure (Figure 9a, b). Wilkawillina and Ajax Limestones with marine archaeocyathids also show local red breccias and paleokarst created during exposure and dissolution (Clarke 1990; Zang 2002). These and other evidence of subaerial exposure have long been documented in these rocks (Mawson & Segnit 1949: Parkin 1969; Stock 1974; Moore 1979, 1990), but the basis for recognising many of the redbeds as paleosols requires further explanation.

Cambrian paleosols pre-date the evolution of vascular plant roots, which are a key feature for recognition of Silurian and younger paleosols (Retallack 1992; Driese *et al.* 1997, 2000), so must be recognised primarily on the basis of soil horizons and soil structures. Soil horizons include observed gradational changes below sharply truncated surfaces (Figure 10), regarded as ancient exposure surfaces because of their more intense weathering and mud cracks, and diffuse zones of carbonate nodules. Gradational change in clay content is superficially like graded bedding (Figures 5a–e, 6b, c), but they are convex rather than concave-linear in grainsize profile and include poorly sorted angular grains (Figure 11a), unlike those of sediment graded by falling through water. Granulometric data for some Cambrian paleosols (Mata and Viparri pedotypes of Figure 12) are comparable with Quaternary loess of sub-Saharan Ghana (Breuning-Madsen & Awadzi 2005), China (Sun *et al.* 2004) and Kansas (median grainsize 4.3–5.6 ϕ, standard deviation 0.9–1.7 ϕ: Swineford & Frye 1951). The poor sorting comes from admixture of well-sorted grains from dust storms with smaller grains from less turbulent air (Sun *et al.* 2004), as well as from breakdown of grains by soil formation (Nemecz *et al.* 2000). Soil formation creates a gradational upward decline in abundance of easily weathered grains such as feldspar and rock fragments, along with an upward increase in weather-resistant minerals such as quartz, and products of weathering such as clay and iron oxides. These mineralogical differences are reflected in gradational chemical changes, particularly those reflecting loss of weatherable base cations (Ca^{2+}, Mg^{2+}, Na^{+}, K^{+}), leaching from barium/strontium ratios, and gleisation from iron oxidation (Figures 5, 6). Petrographic evidence of hydrolytic weathering includes ferruginous clayey pellicles (argillans) of mixed-layer smectite–illite around feldspar and rock fragments (Figure 11d), and mixtures of fresh and weathered grains (Stock 1974).

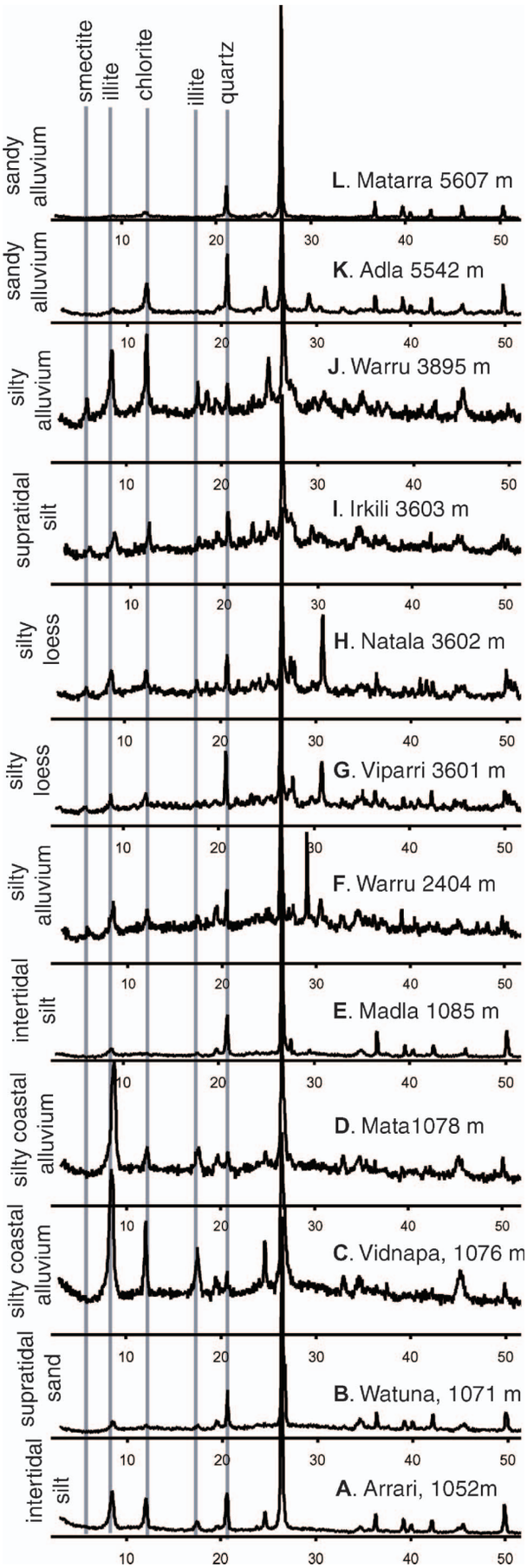

Evidence for soil oxidation of iron in well-drained paleosols includes even distribution of hematite pigment in carbonate-cemented siltstones (Figure 11e), sharp boundaries between red and green beds (Figure 10d), mottles only a few millimetres thick within texturally homogenous siltstones (Figure 11e), and red clasts at the base of green-grey paleochannel sandstones (Figure 9c) (Stock 1974; Moore 1990).

Distinctive soil structures of the paleosols include nodules of micrite (Figure 11f), rosettes of anhydrite (replacing gypsum: Figure 11g) and calcite geodes pseudomorphous after gypsum rosettes (Figure 9d). Micritic nodules show remnant quartz grains within replacive fabrics (Figure 11f), as well as cracks filled with spar supporting rotated soil clasts (displacive fabrics), indicating formation under low confining pressures (Figure 11b). Both are typical microfabrics of soil carbonate (caliche), as are the observed progression of carbonate horizon development from calcareous mottles to hard carbonate nodules of increasing size, then benches, as in aridland soils today (Gile *et al.* 1966, 1980). The development of gypsum can be similar because some original rosettes also show relict quartz and other grains as evidence of replacement of prior silty matrix (Figure 11c). Gypsum and halite are soluble in outcrop, and may also have been soluble in Cambrian paleosols, as indicated by halite hopper casts in intertidal paleosols (Figure 9a). The inbowed concentric margins of the hopper casts represent episodic progress of halite dissolution near the land surface, where the growing gap between matrix and crystal is filled with sediment (Brooks 1955). The empty centres of geode-like calcite nodules with crystal impressions also may have been dissolved of their likely gypsum or other salts during the Cambrian or subsequently (Figure 9d).

The most spectacular soil structures are deep cracks and ridges characteristic of the Viparri pedotype (Figure 10a, b), and interpreted as vertic structure (mukkara) of a swelling clay soil (Vertisol). Unlike gravity-driven load structures or mud volcanoes (Owen 2003), or seismically induced sand blows, contorted lamination, dykes and breccia (Wheeler 2002), this distinctive deformation fades downward from an undulating, erosionally truncated surface to undeformed layers. The ridged cracks are exposed in bedding planes as well as vertical faces, and are most like linear gilgai (Paton 1974). The origin of this ancient ridged microrelief is thus interpreted as evidence of shrink-swell and thixotropy, distinctive of seasonally dry, swelling clay (smectite-rich), soils (Vertosols of Isbell 1998; Vertisols of Soil Survey Staff 2000).

PALEOSOL DIVERSITY

Paleosols are abundant in Cambrian rocks of South Australia: 396 successive paleosols were seen in Ten

Figure 8 Clay mineral variation of Cambrian paleosols on X-ray diffractometer traces with depth of burial, pedotype and sedimentary paleoenvironment in the central Flinders Ranges.

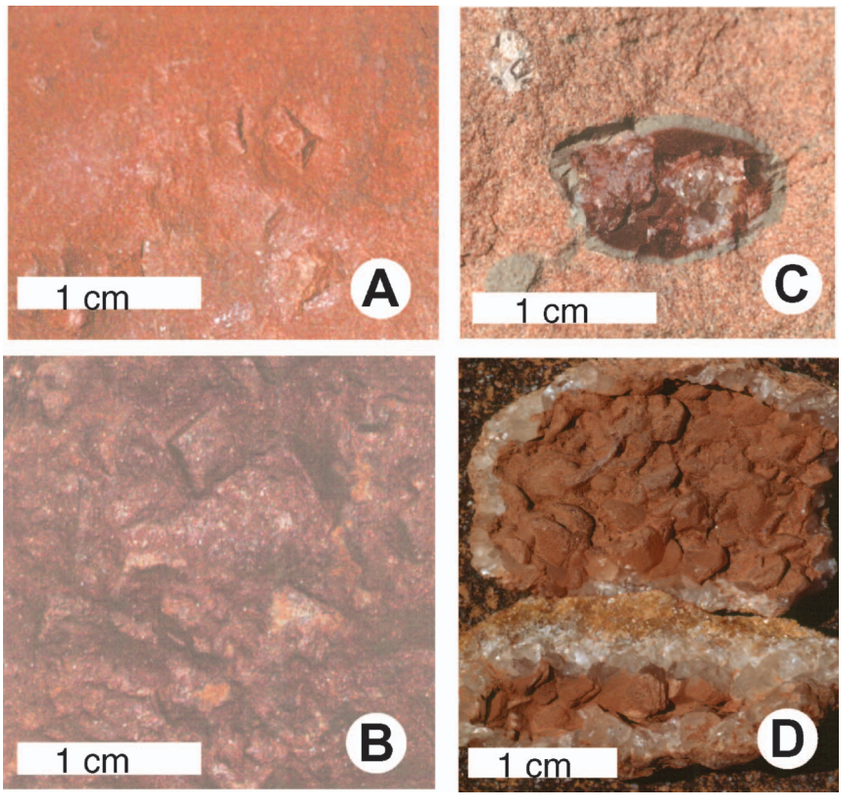

Figure 9 Hand specimens of Cambrian paleosols. (a, b) Halite-crystal hopper-casts in Imba pedotype of Billy Creek Formation near upper Balcoracana Creek trilobite locality of Pocock (1970: correlates with 2470 m in Figure 2a) (a, R3415A; b, R3415B). (c) Calcite and red claystone clast with narrow (2 mm) grey-green reduction halo in paleochannel of Moodlatana Formation (3560 m in Figure 2a) (R3386). (d) Ellipsoidal calcite geode, pseudomorphous after gypsum, broken open horizontally (above) and vertically (below), in Irkili pedotype of lower Balcoracana Formation (3611 m in Figure 2a) (R3327). 'R' numbers are specimen numbers in author's research collection: see Figures 5, 6.

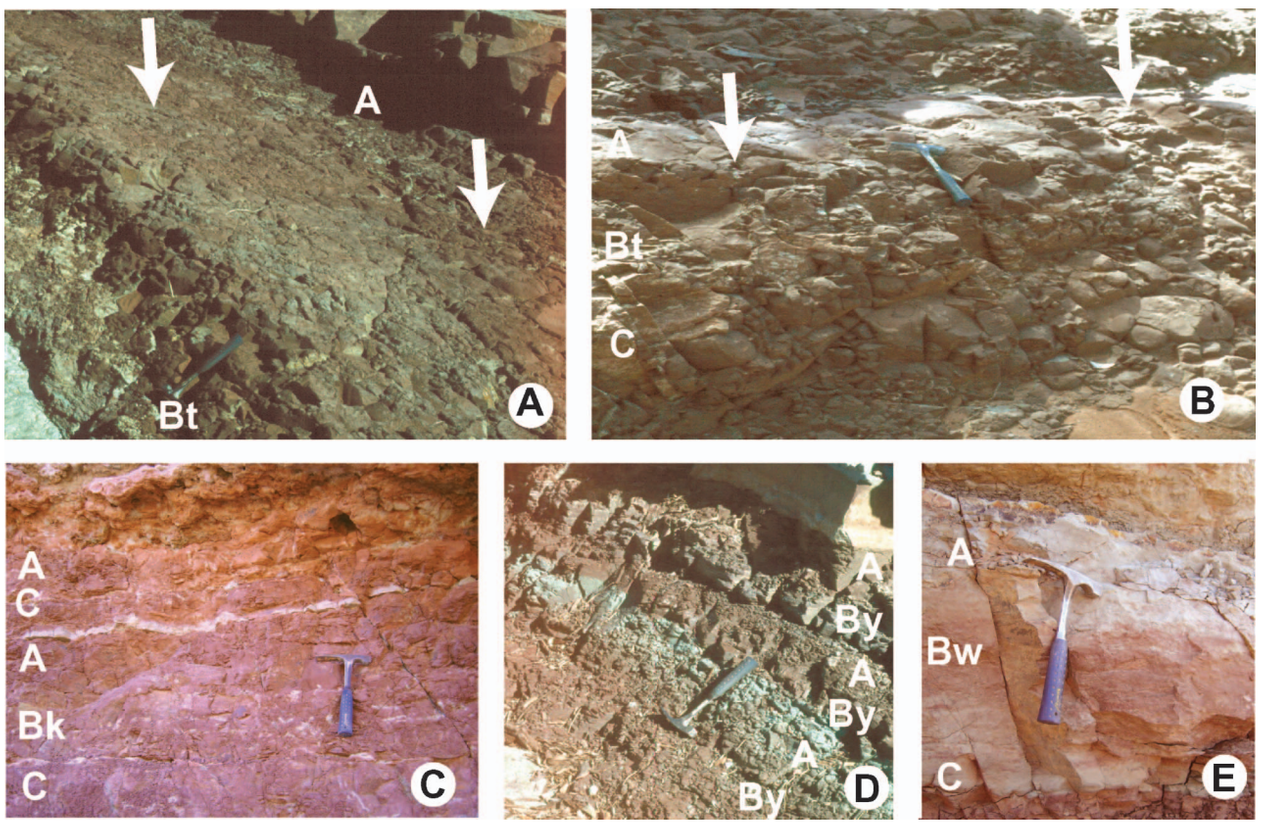

Figure 10 Field photographs of Cambrian paleosols. (a, b) Type Viparri silty clay loam paleosol bedding plane exposure of surface (a) and profile form (b) in upper Moodlatana Formation (3603 m in Figure 2a). (c) Type Imba clay and Warru clay loam paleosols in upper Billy Creek Formation (2404 m in Figure 2a). (d) Irkili paleosol in lower Balcoracana Formation (3611 m in Figure 2a). (e) Type Mindi silty clay paleosol in upper Moodlatana Formation (3605 m in Figure 2a). All photographs are along Ten Mile Creek north of a big bend at 31.25736°S, 138.94142°E (a, b, d, e) and a steep bank at 31.28414°S, 138.91899°E (c).

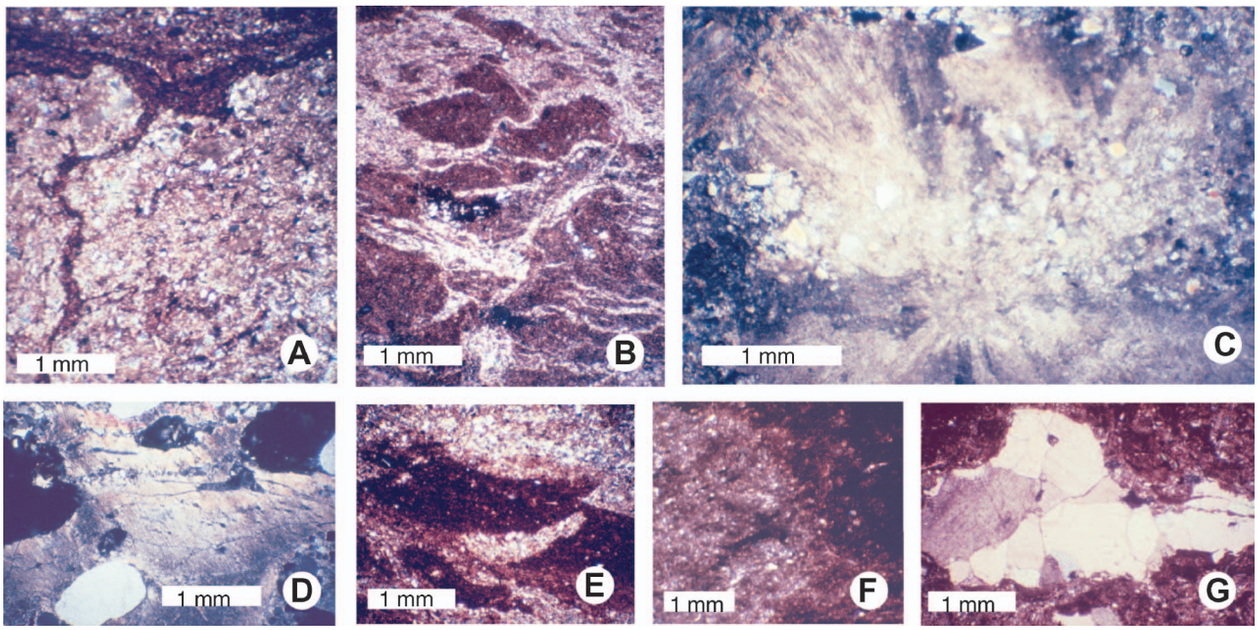

Figure 11 Photomicrographs of Cambrian (–Ordovician?) paleosols. (a) Loessic, poorly sorted, angular siltstone and ptygmatically folded desiccation crack in A horizon of Natala paleosol, upper Moodlatana Formation (3602 m in Figure 2a) (R3315). (b) Hyperdisplacive carbonate cement with rotated clasts of matrix in A horizon of Imba paleosol, upper Billy Creek Formation (2404 m in Figure 2a) (R3371). (c) Replacive selenite (acicular gypsum) rosette in By horizon Matarra paleosol, lower Grindstone Range Sandstone (5612 m in Figure 2a) (R3359). (d) Clay coating (illuviation argillan) in A horizon of Arrari paleosol, lower Parachilna Formation in Parachilna Gorge (correlates with 1052 m in Figure 2a) (R3281). (e) Curled clay flake from desiccation crack in C horizon of Natala paleosol upper Moodlatana Formation (3602 m in Figure 2a) (R3319). (f) Replacive micrite nodule (left) and oxidised matrix (right) in Warru paleosol, upper Billy Creek Formation (2403 m in Figure 2a) (R3376). (g) Blocky anhydrite replacing small gypsum rosette in type Mindi paleosol, upper Moodlatana Formation (3605 m in Figure 2a) (R3333). 'R' numbers are specimen numbers in author's research collection: see Figures 5, 6.

Mile Creek within 836 m of exposed non-marine facies. There are more than 2400 paleosols in the non-marine 3600 m of that section assuming comparable abundance in unexposed sequences: this is an underestimate because paleochannel sandstones crop out better than clayey paleosols, as is clear from the abundance of paleosols in the Lake Frome cores. The abundance and diversity of paleosol features can be brought to order by recognising 17 different kinds, or pedotypes, each with a distinctive suite of pedogenic features. Each pedotype reflects a different suite of formative conditions which are thus open for interpretation, and was named for distinctive features using the Adnamatna local language (McEntee & McKenzie 1992) (Figures 2, 5, 6; Table 1). All pedotypes in the Parachilna Formation (Arrari, Vidnapa, Mata, Watuna, Yanga, Madla) have trace fossils (*Skolithos, Diplocraterion*) and other indications of marine influence, but none show halite hopper casts, gypsum or chemical salinisation (Figure 6). *Diplocraterion* and *Skolithos* in Parachilna Formation paleosols are also ferruginised and encrusted with clay, so pre-dated or were coeval with soil formation, unlike grey-green, pyritic, marine trace fossils formed in red Ordovician paleosols formed by marine transgression over a well-drained soil (Driese & Foreman 1991, 1992). Parachilna Formation paleosols also lack geode-pseudomorphs of gypsum (Figure 9d), hopper casts of halite (Figure 9a, b), displacive gypsum (Figure 11g) and chemical salinisation (Figure 5) of Imba, Mindi and Irkili pedotypes of the Billy Creek, Moodlatana and Balcoracana Formations, which also show local flaser bedding and trackways suggestive of marine influence (Parkin 1969; Moore 1990). Replacive gypsum (Figure 11c) is found in the Matarra pedotype of the Grindstone Range Sandstone, where associated sedimentary facies are fluviolacustrine quartz sandstone (Stock 1974). Other pedotypes (Adla, Natala, Upi, Viparri, Wandara, Warru, Wilpi) are in fluvial facies of weakly bedded, red, floodplain deposits and thick paleochannel sandstones. Trace fossils and associated sedimentary facies are thus guides to varying degrees of marine *vs* fluvial influence.

Each field pedotype can be identified in modern soil classifications using petrographic and geochemical data for its type profile (Figures 5, 6). Classifications of the United States (Soil Survey Staff 2000), United Nations Educational and Scientific Organization (FAO 1974), and traditional names (Stace *et al.* 1968) can be used (Table 2), but the following paragraph is written from the perspective of the current Australian classification (Isbell 1998: McKenzie *et al.* 2004). Many of the paleosol profiles (Imba, Matarra, Wandara, Watuna, Wilpi, Yanga) show minimal soil development with many remaining sedimentary structures, as in Rudosols, which are divided according to sandy or silty texture and degree of layering. These paleosols preserve little imprint of climate or other long-term influences on soil formation (Table 2). Other paleosols with limited paleoclimatic implications include those with drab mottles (Ararri, Madla, Upi) indicative of waterlogging, as in Hydrosols, and other paleosols (Mindi) with weak

Table 1 Cambrian pedotype derivation, diagnosis and classification.

Pedotype name	Adnamatna meaning	Diagnosis	US soil taxonomy (Soil Survey Staff 2000)	Food and Agriculture Organization (FAO 1974)	Traditional Australian (Stace *et al.* 1968)	Australian (Isbell 1998; McKenzie *et al.* 2004)
Adla	Fire	Red sand (A) over shallow (<50 cm) calcareous nodules (Bk)	Haplocalcid	Calcic Xerosol	Red calcareous soil	Calcic Calcarosol
Arrari	Green	Green siltstone (A) with *Diplocraterion* and *Monocraterion* over calcareous mottles (Bk)	Endoaquept	Calcaric Gleysol	Humic gley	Intertidal Hydrosol
Imba	Ash	Thin green mottles (A) in red shale	Fluvent	Calcaric Fluvisol	Alluvial soil	Stratic Rudosol
Irkili	Salt	Green mottles (A) over red shale with calcite geodes after gypsum (By)	Calcigypsid	Gypsic Xerosol	Solonchak	Salic Hydrosol
Madla	Mud	Green sandstone with *Diplocraterion* A) over brown siltstone (Bw)	Fluvaquentic Endoaquept	Gleyic Cambisol	Humic gley	Extratidal Hydrosol
Mata	Thick	Red siltstone (A) with rare *Skolithos* over deep (>50 cm) calcareous nodules (Bk)	Vertic Haplocalcid	Calcic Xerxosol	Red clay	Brown Dermosol
Matarra	Hard salty	Red sand (A) above shallow (<20 cm) crystals of gypsum (By)	Natrigypsid	Gleyic Solonchak	Solonchak	Hypergypsic Rudosol
Mindi	Net	Grey-red mottled siltstone (A)	Aeric Endoaquept	Gleyic Cambisol	Wiesenboden	Brown Orthic Tenosol
Natala	Big	Red siltstone (A) over deep (>50 cm) calcareous nodules (Bk)	Veric Haplocalcid	Calcic Cambisol	Red clay	Brown Dermosol
Upi	Blood	White sand with red burrows (*Thalassinoides*) and bedding (A)	Oxyaquic Quartzi-psamment	Dystric Fluvisol	Siliceous dand	Redoxic Hydrosol
Vidnapa	Little	Red sandy siltstone (A) with *Skolithos* over shallow (<50 cm) calcareous nodules (Bk)	Haplocalcid	Calcic Erosol	Red calcareous soil	Calcic Calcarosol
Viparri	Thick	Red siltstone (A) with pseudo-anticlinal sandy layers over deep (>50 cm) calcareous nodules (Bk)	Vertisol	Chromic Vertisol	Red clay	Brown Vertosol
Wandara	Sand	Ferruginised sandstone (A)	Psamment	Dystric Fluvisol	Siliceous dand	Arenic Rudosol
Warru	Red clay	Red clayey siltstone (A) over shallow (<50 cm) calcareous nodules (Bk)	Haplocalcid	Calcic Xerosol	Red calcareous soil	Calcic Calcarosol
Watuna	Burrow	Red sandstone (A) with abundant *Skolithos*	Psamment	Calcaric Fluvisol	Calcareous sand	Arenic Rudosol
Wilpi	Dried skin	White sandstone with elephant skin and carpet texture (A)	Quartzi-psamment	Dystric Fluvisol	Siliceous sand	Arenic Rudosol
Yanga	Liver	Thin (<20 cm) purple sandstone (A) with *Skolithos*	Psamment	Calcaric Fluvisol	Calcareous sand	Lutic Rudosol

soil mixing, as in Tenosols. Cambrian landscapes also included climatically significant soils with blocky-structured, though texturally indistinct, subsurface (B) horizons (Mata, Natala), as in Dermosols, well-formed calcareous nodules (Adla, Warru), as in Calcarosols, and evidence of shrink-swell behaviour (Viparri), as in Vertosols. Dermosols, Calcarosols and Vertosols today are well-developed soils of dry and seasonal climates (McKenzie *et al.* 2004), and have specific features, such as depth to calcic horizon, which can be quantitative indications of paleoclimate (Retallack 2001).

PALEOTOPOGRAPHY

All the Cambrian paleosols formed in low-relief sedimentary environments of intertidal mudflats and riverine bottomlands (Wopfner 1970; Stock 1974; Moore 1990), but minor differences in location with respect to the water-table are apparent from soil structure, calcareous nodules, red *vs* green color, and iron oxidation states of the paleosols (Figures 5, 6) and these can be related to different sedimentary facies to reconstruct alluvial and coastal paleotopography.

The Lower Cambrian Parachilna and underlying Uratanna Formations fill paleovalleys with about 200 m of paleorelief into underlying sandstones (Mount 1989; Zang 2002). Coastal depositional surfaces of the Parachilna Formation include grey-green paleosols (Arrari) interpreted as mostly waterlogged, and mottled paleosols (Madla), interpreted as intermittently waterlogged estuarine sediment (Figure 12b). Arrari profiles have thin iron-stained horizons and illuviated clay skins (Figure 11d) but are mainly grey-green like other

Table 2 Cambrian pedotype interpretation.

Pedotype	Paleoclimate (mean annual temperature and rainfall)	Former biota	Paleotopography	Parent material	Formation time (years)
Adla	Semiarid (378 ± 35 mm), cool (13.7 ± 4.4°C)	Biological soil crust	Low alluvial terrace and floodplain	Quartz-rich sand	6800 ± 3800
Arrari	Semiarid (390 ± 35 mm)	Microbial mat with worms (*Monocraterion*)	Interidal sand flat	Quartzo-feldspathic sand	10–200
Imba	Not relevant	Microbial mat	Supratidal and alluvial mud flat	Quartzo-feldspathic silt, volcanic tuff	5–10
Irkili	Semiarid (324 ± 78 mm), cool (8.5 ± 4.4°C)	Microbial mat	Supratidal and alluvial mud flat	Quartzo-feldspathic silt	1000–2000
Madla	Subhumid (909 ± 182 mm), cool (9.0 ± 4.4°C)	Microbial mat with worms (*Skolithos, Diplocraterion*)	Supratidal sand flat	Quartzo-feldspathic sand	100–500
Mata	Subhumid (551 ± 104 mm), cool (10.0 ± 4.4°C)	Biological soil crust, rare worms (*Skolithos*)	Low alluvial terrace and floodplain	Quartzo-feldspathic loess and sand	11 000 ± 3200
Matarra	Arid (100–300), high evapotranspiration	Microbial mat	Floodplain playa lake	Quartz-rich sand	100–500
Mindi	Not relevant	Microbial mat	Supratidal	Quartzo-feldspathic silt	5–10
Natala	Subhumid (551 ± 36 mm), cool (8.1 ± 4.4°C)	Biological soil crust	Low alluvial terrace and floodplain	Quartzo-feldspathic silt and sand	500–2000
Upi	Not relevant	Biological soil crust with worms (*Thalassinoides*)	Alluvial levee and point bar	Quartz-rich sand	5–10
Vidnapa	Semiarid (456 ± 39 mm), cool (9.6 ± 4.4°C)	Biological soil crust, rare worms (*Skolithos*)	Supratidal creek upper levee	Quartzo-feldspathic sand and loess	7300 ± 900
Viparri	Subhumid (599 ± 48 mm), marked dry season, cool (8.2 ± 4.4°C)	Biological soil crust	Low alluvial terrace and floodplain	Quartzo-feldspathic loess and sand	8800 ± 3400
Wandara	Not relevant	Biological soil crust	Alluvial levee and point bar	Quartzo-feldspathic sand	5–10
Watuna	Not relevant	Microbial mat, with worms (*Skolithos*)	Supratidal sand flat	Quartzo-feldspathic sand	22 500 ± 12 800
Warru	Semiarid (426 ± 50 mm), cool (9.7 ± 4.4°C)	Biological soil crust	Low alluvial terrace and floodplain	Quartzo-feldspathic loess and sand	6600 ± 5400
Wilpi	Not relevant	Biological soil crust	Alluvial levee and point bar	Quartz-rich sand	5–10
Yanga	Not relevant	Microbial mat, with worms (*Skolithos*)	Supratidal creek lower levee	Quartzo-feldspathic sand	5–10

intertidal Cambrian paleosols (Álvaro *et al.* 2003). Other paleosols of the Parachilna Formation are red, with clay skins, slickensided cracks, calcareous nodules, and deeply penetrating burrows interpreted here as evidence of land surfaces some 30 cm (Yanga), 50 cm (Watuna,Vidnapa) to 1 m (Mata) above permanent water-table. Mata paleosols show significant accumulation of pedogenic clay and loess, distinct from its own estuarine sediment parent and wholly estuarine paleosols (Madla of Figure 12). In the sandy estuarine depositional environment of the Parachilna Formation, these various pedotypes may have formed different geomorphic surfaces of intertidal to supratidal flats.

The Lower–Middle Cambrian Billy Creek, Moodlatana and Balcoracana Formations have been reconstructed as a linear clastic shoreline of low relief, flanking low hills of the Gawler Craton to the west (Wopfner 1970; Moore 1990). Associated stromatolitic and other algal limestones, as well as flaser-bedded parent materials, suggest that Irkili, Imba and Mindi pedotypes were formed on tidal flats, though all are red and some show clay skins and cracks extending as deep as 30 cm, as in high supratidal flats. Without mangrove or salt marsh vegetation to stabilise and raise shorelines by sediment baffling in the Cambrian, tidal influence may have extended further inland than is usual today. Fluvial facies of red floodplains and grey-green, trough cross-bedded, paleochannels are rare in the Billy Creek and Balcoracana Formations, but common in the Moodlatana Formation. Closely associated with

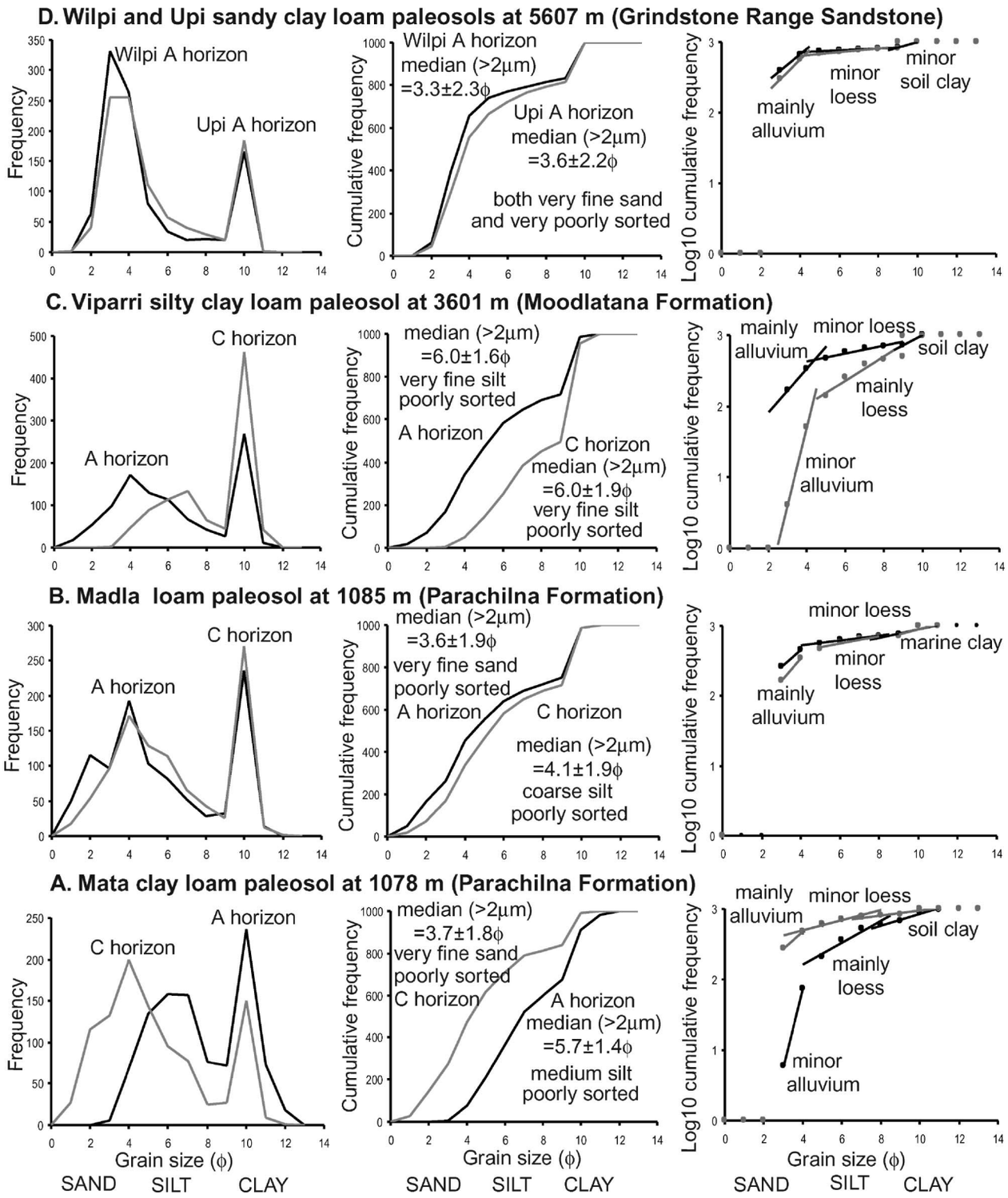

Figure 12 Granulometric analysis of selected Cambrian (–Ordovician?) paleosols of the Flinders Ranges, each from 1000 measurements of grain long axes, using an ocular micrometer in a petrographic microscope.

sandstone paleochannels are thick red sandy paleosols with much relict bedding (Wandara), here interpreted as well-drained soils of levee tops and other frequently disturbed areas. Clayey bedded paleosols (Imba) are also associated with paleochannels but are less deeply cracked and oxidised (<20 cm), and may represent swales within the channel tract of loosely sinuous rivers. Other paleosols with large calcareous nodules, clay skins and other soil structure (Natala, Viparri, Warru) represent land surfaces well drained to depths of more than 50 cm (Warru) and more than 1 m (Natala, Viparri). Viparri paleosols had cumulic alluvial additions, much deformed at the surface, to their loess parent material (Figure 12c).

Pedotype diversity is more limited in the red Pantapinna Sandstone and overlying white Grindstone Range Sandstone (Figure 2d), which have been interpreted as fluvial (Stock 1974; Moore 1990) or intertidal (Gravestock 1995). No tidal facies or trace fossils were seen in paleochannels and paleosols of the Pantapinna Sandstone in Ten Mile or Balcoracana Creeks. Weakly developed sandy (Wandara), sandy calcareous nodular (Adla, Natala) and clayey calcareous paleosols (Warru) of the Upper Cambrian Pantapinna Sandstone may represent disturbed levees and stable sandy and clayey floodplains, respectively. Similar paleosols (Wandara, Adla, Natala) persist into the Upper Cambrian or Lower Ordovician (?) Grindstone Range Sandstone, where gypsiferous paleosols (Matarra) and elephant-skin textured sandstones (Wilpi) may represent playa lakes and their margins on sandy floodplains. Trace fossils comparable with *Palaeophycus* may indicate some marine influence. White sandstone with red-clay-filled burrows (Upi), represent soils of waterlogged streamside environments accumulating oxidised dust only at the surface and in open burrows. Despite evidence of dry climate and sandy sediment, no eolian dunes were found in any of these formations.

PARENT MATERIAL

Pedotypes of the Parachilna Formation are different from those of other formations in part because of their distinctive parent materials: an even textural mix of sand, silt and clay, and chemically low alkalies and alkaline-earths (Ca, Mg, Na and K). The Parachilna Formation fills paleorelief of at least 200 m (Zang 2002), and has a component of recycled material, weathered during earlier depositional cycles (Figure 6). Volcanic ash in the Billy Creek Formation (Haines & Flöttmann 1998) is a parent material of the lower part of the formation, evident from devitrified shards and pervasively displacive micrite after imogolite precursors of smectite, now illitised, as in other volcaniclastic paleosols (Retallack 1991a; Retallack *et al.* 2000). The upper Billy Creek, Moodlatana and Balcoracana Formations show little evidence of volcanic ash, and have a quartzofeldspathic composition with much clay and also large amounts of loess (highly angular eolian silt: Figure 12b). Parent materials of paleosols in the Pantapinna and Grindstone Range Sandstones also are quartzo-feldspathic, but very sandy and with little clay. The grainsize distributions of Grindstone Range Sandstone paleosols (Figure 12d) are alluvial, not loess.

LANDSCAPE STABILITY

Sedimentary environments are by their nature unstable and sedimentary processes work to undo the steady and relentless work of soil formation. The various pedotypes differ substantially in degree of soil development and corresponding degree of destruction of sedimentary structures. Pedotypes with remnants of bedding (Imba, Upi, Wandara, Yanga, Wilpi) represent young soils, little modified from their sedimentary parent material of sand, silt and clay. Other pedotypes have the hackly structure of clay skins and colour mottles indicating substantial mixing in place by shrink-swell, cracking and possible biotic effects over a considerable period of time (Mindi). Many other paleosols have in addition to these indications of soil mixing such features as gypsum-rich subsurface horizons (Irkili, Matarra) and calcareous nodules (Adla, Mata, Vidnapa, Warru). Duration of formation of modern soils (A in 10^3 y) is related to calcareous nodule diameter (N in mm), by Equation 1 ($R^2 = 0.57$; SE $= \pm 1.8 \times 10^3$ y) derived from radiocarbon dating of soils (Retallack 2005).

$$A = 3.92N^{0.34} \quad (1)$$

Calculations of Cambrian soil duration from this equation (Figure 13e) show generally short times ($<10\,000$ y) of soil formation with exceptions in the earliest, middle and latest Cambrian. This was not an ephemeral and unstable landscape, but one of local stability.

PALEOCLIMATE

Several features of soils are significantly related to climatic variables, and can be used to infer paleoclimate from paleosols, after appropriate adjustment for alteration after burial. Mean annual precipitation (R in mm) is related to depth to carbonate nodules in the soil (D_o in cm: Equation 2 with $R^2 = 0.52$; SE $= \pm 147$ mm: Retallack 2005). Thickness of the soil with carbonate (H_o in cm) also increases with mean annual range of precipitation, defined as the difference of means between wettest and driest months (M in mm: using Equation 3 with $R^2 = 0.58$; SE $= \pm 22$ mm: Retallack 2005). Original depth to carbonate nodules (D_o) and thickness of carbonate soil (H_o) before burial compaction were derived from paleosol measurements (D_p or H_p) using estimated depth of overburden (K in km) in a standard compaction algorithm (Equation 4: from Sheldon & Retallack 2001) for 0.6 km plus stratigraphic level in the observed sequence (Figure 2). Burial compaction to $82 \pm 6\%$ of original length was measured directly from ptygmatic folding of five clastic dykes in the Warru silty clay loam paleosol at 3605 m in the Ten Mile Creek section, where Equation 4 gives a compaction of 81%. Depth and spread of carbonate in the paleosols was not corrected for higher than modern atmospheric CO_2, because the increase from 280 to 3080 ppm V has been modelled (McFadden & Tinsley 1985) to cause a minor (5 cm) increase in depth to pedogenic carbonate.

$$R = 137.24 + 6.45D_o - 0.013D_o^2 \quad (2)$$

$$M = 0.79H + 13.71 \quad (3)$$

$$D_o = D_p/[-0.51/\{0.49/(e^{0.3K})\} - 1] \quad (4)$$

Other paleoclimatic variables come from chemical analysis of paleosols. The chemical index of alteration

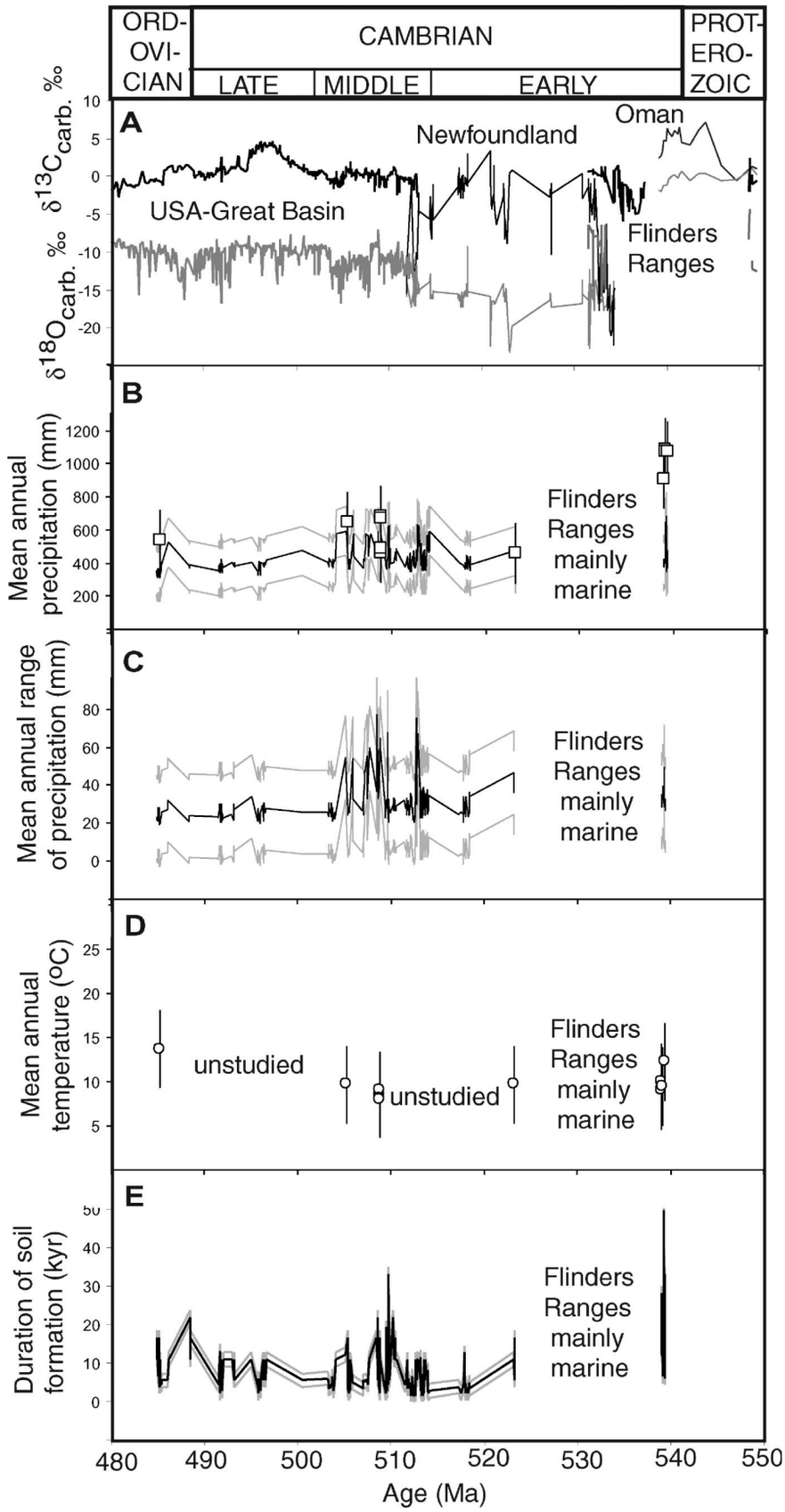

Figure 13 Time series of Cambrian paleoenvironmental change. (a) Stable isotopic values of carbon and oxygen from marine limestones of the Great Basin, USA (Saltzman 2005), Newfoundland, Canada (Brasier *et al.*1992), Flinders Ranges, South Australia (Tucker 1991; Surge 1996; Calver 2000), and Oman (Fike *et al.* 2006). (b) Mean annual precipitation (mm) in South Australia from compaction-corrected depth to calcic horizon (heavy line with flanking error from standard error of transfer function) and from chemical index of alteration without potash (open squares with standard error from transfer function). (c) Mean annual range of precipitation (mm) in South Australia from compaction-corrected thickness of paleosols with calcareous nodules (error from standard error of transfer function). (d) Mean annual temperature (°C) in South Australia estimated from salinisation index of paleosols (error from standard error of transfer function). (e) Duration of soil formation in South Australia calculated from size of calcareous nodules in paleosols.

[$C = 100.mAl_2O_3/(mAl_2O_3 + mCaO + mMgO + mNa_2O)$, in moles] increases with mean annual precipitation (R in mm) in modern soils (Equation 5 with $R^2 = 0.72$; SE $= \pm$ 182 mm: Sheldon *et al.* 2002). Paleotemperature can be derived from salinisation [$S = (mK_2O + mNa_2O)/mAl_2O_3$, in moles] which decreases with mean annual

temperature (T in °C: using Equation 6 with $R^2 = 0.37$; SE = ± 4.4°C: Sheldon *et al.* 2002).

$$R = 221e^{0.0197C} \quad (5)$$

$$T = -18.5S + 17.3 \quad (6)$$

Results of these calculations for Cambrian paleosols show considerable paleoclimatic variation, particularly in the middle and earliest Cambrian (Figure 13b–d). Precipitation was mostly semiarid, but there were spikes of subhumid precipitation in the earliest Cambrian, then at five separate levels in the middle Cambrian, and in what may be the earliest Ordovician (Figure 13b). All of these were times of marine transgression in South Australia (Bengtson *et al.* 1990; Zang 2002; Jago *et al.* 2006). These subhumid spikes also correlate with negative excursions in $\delta^{18}O$ and $\delta^{13}C$ in marine carbonates (Figure 13a) in the Flinders Ranges (Calver 2000; Tucker 1991) and overseas (Brasier *et al.* 1992; Fike *et al.* 2006).

Both chemical and calcic indications of precipitation are in agreement for most of the record, but diverge considerably in the Parachilna Formation, which is chemically weathered more profoundly than indicated by depth to calcic horizon in paleosols. Parachilna Formation paleosols may have developed on material redeposited from pre-existing more deeply weathered paleosols at the disconformable Precambrian–Cambrian boundary. Only a few of the subhumid levels in the Middle Cambrian show monsoonal levels of mean annual range of precipitation: other levels show modest seasonality of precipitation (Figure 12c). Mean annual temperature calculated from salinisation is temperate (8–14 ± 4.4°C) rather than tropical expected from a paleolatitude of about 20°N (Jago *et al.* 2002). Data on paleotemperature are sparse (Figure 12d) because each estimate requires a full chemical analysis, and may be compromised by a Cambrian weathering regime of alkalies different from that in modern soils (Basu 1981).

LIFE ON AND IN LAND

Intertidal–supratidal paleosols of the Parachilna Formation show variations in abundance and diversity of trace fossils that may reflect different degree of marine influence in coastal soils. Diverse assemblages of trace fossils including the definitively marine *Diplocraterion* (Figure 14a at arrow) and the likely marine *Monocraterion* are found in Ararri and Madla paleosols. Ararri paleosols have a grey-green colour and chemical gleisation characteristic of persistently waterlogged soils, but Madla has an oxidised horizon, perhaps due to intermittent or subsequent exposure (Figure 6). Simple vertical burrows of *Skolithos* (Figure 14a) are abundant in some Cambrian paleosols (Yanga, Watuna, Vidnapa) and sparse in other paleosols (Mata) of the Parachilna Formation. In all paleosols with *Skolithos*, these burrows penetrate to the base of oxidised surface layers

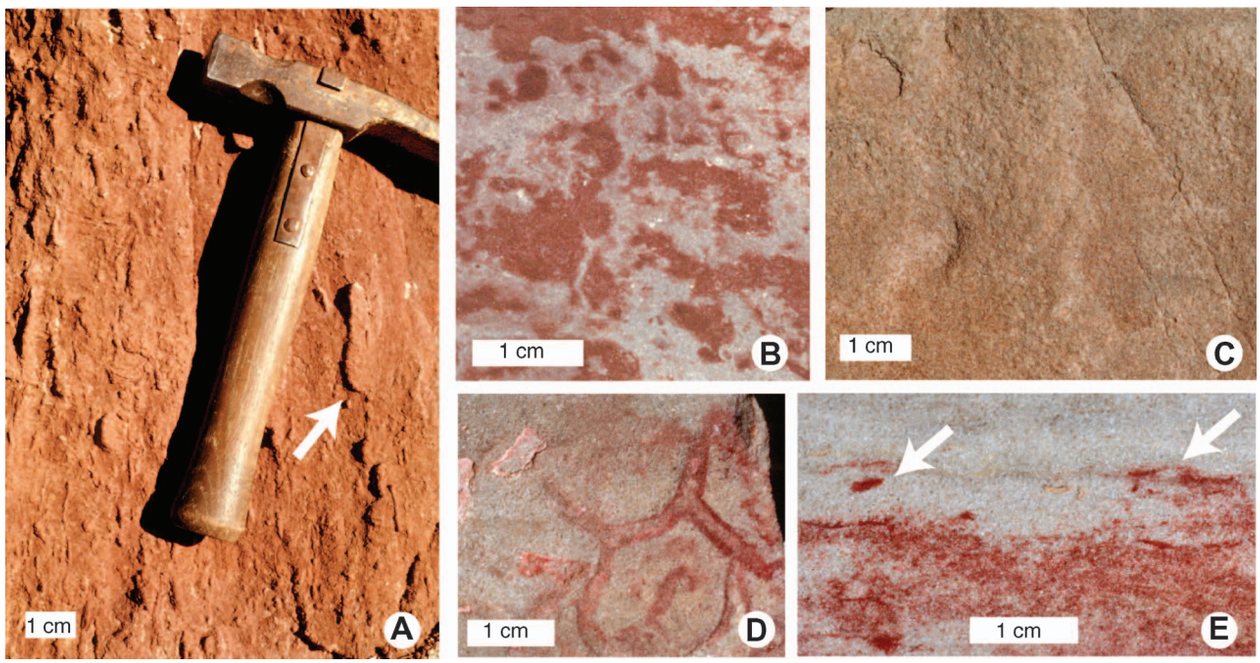

Figure 14 Trace fossils in Cambrian and Ordovician (?) paleosols. (a) *Diplocraterion* (at arrow) and *Skolithos* in Bw horizon of Madla paleosol, Parachilna Formation in Brachina Gorge (correlates with 1060 m in Figure 2a) (31.34067°S, E139.55194°E). (b) Drab-haloes (grey) around filaments (light grey) in red soil matrix (dark), here interpreted as biological soil crust, A horizon of type Mindi paleosol, upper Moodlatana Formation (3605 m in Figure 2a) (P422357). (c) Pustulose ('carpet') and healed-crack ('old elephant skin') textures interpreted as biological soil crust on sandstone surface of Wilpi paleosol, Grindstone Range Sandstone (5613 m in Figure 2a) (P42260). (d, e) bedding-plane exposure (d) (P42258) and cross-sections (e) (P42259) of shallow burrows (*Thalassinoides*), A horizon Upi paleosol, Grindstone Range Formation (5612 m in Figure 2a). 'P' numbers are South Australian Museum specimen numbers.

(as much as 70 cm in Mata pedotype) into unoxidised layers below. This observation can be interpreted as evidence that the *Skolithos*-forming animal was aquatic, burrowing as far as necessary to the water-table in order to avoid desiccation in dry parts of the soil, in a similar manner to crayfish in floodplain soils today (Hasiotis & Mitchell 1993). Other aquatic protistans and bacteria also can be expected to have colonised water-tables of coastal soils at depths of up to a metre below the exposed surface. *Skolithos* is common in waterlogged freshwater paleosols of post-Devonian age (Retallack 1976), but abundance of *Skolithos* in the coastal Parachilna Formation and its absence in fluvial Moodlatana, Pantapinna and Grindstone Range Formations, is circumstantial evidence that the Cambrian *Skolithos*-forming animal was marine.

The most common likely biogenic structures in these Cambrian paleosols of both supratidal and fluvial paleoenvironments are grey-green tubular features at the very top of the profiles (Figure 14b), similar to drab-haloes common around root traces in Devonian and geologically younger paleosols (Retallack 1997a). In post-Silurian paleosols, drab haloes are thought to form by burial gleisation of the organic matter of a buried root (Retallack 2001), because the haloes scale closer to volume of the root (πr^2 in exposed surface) than surface area ($2\pi r$) of the root (Figure 15). Cambrian drab-haloes from South Australia are small (mean and standard deviation 1.73 ± 0.78 mm diameter) with a slender central hole of the original filaments now filled with clay (0.56 ± 0.29 mm diameter). In contrast, Triassic drab haloes are large (6.46 ± 3.74 mm around root traces 1.44 ± 0.85 mm: Retallack 1976, 1997b) and Eocene drab haloes are similar (halo 5.47 ± 2.48 mm around root 1.54 ± 0.78 mm: Retallack *et al.* 2000). Polymodal haloes in Cambrian paleosols may represent several species of organisms, whereas Triassic and Eocene samples were from limited areas (~ 1 m^3) of forested paleosols, perhaps formed by a single tree. Drab tubular features comparable with the Cambrian examples are also documented in 1.8 Ga alluvial paleosols of the Lochness Formation of Queensland (Driese *et al.* 1995), so pre-date the Cambrian. Cambrian and Proterozoic drab-haloed filaments are most like rhizomorphs of lichens and bundles of cyanobacteria in modern biological soil crusts, where microbes are in intimate association with sediment, unlike intertidal mats which cover sediment (Belknap *et al.* 2000). In the plant formation terminology of Retallack (1992), biological soil crusts include microbial earths and rocklands, with entirely microscopic organisms, as well as polsterlands, with larger organisms such as lichens, mosses and liverworts. With a diameter of 0.56 mm, the Cambrian examples (Figures 14b, 15a) may have been lichen, moss or liverwort polsterlands.

Other biogenic sedimentary structures in sandstone are distinctive fabrics of narrow cracks and mounds (elephant skin texture), and small protuberances (carpet texture: Figure 13c). Both textures are comparable with biological soil crusts, which bind loose sand so that it behaves like clay, expanding with wetting, contracting with drying, and then filled in by protuberance of filamentous organisms (Belknap *et al.* 2000). This kind of pustulose, mounded and narrowly cracked surface found on the Lower Ordovician (?) Wilpi pedotype is distinct from smooth to striated and wrinkled intertidal microbial mats, which cover rather than mix into underlying sediment, and are transparent, in the sense that underlying sedimentary structures are not obscured (Hagadorn & Bottjer 1997; Pruss *et al.* 2004).

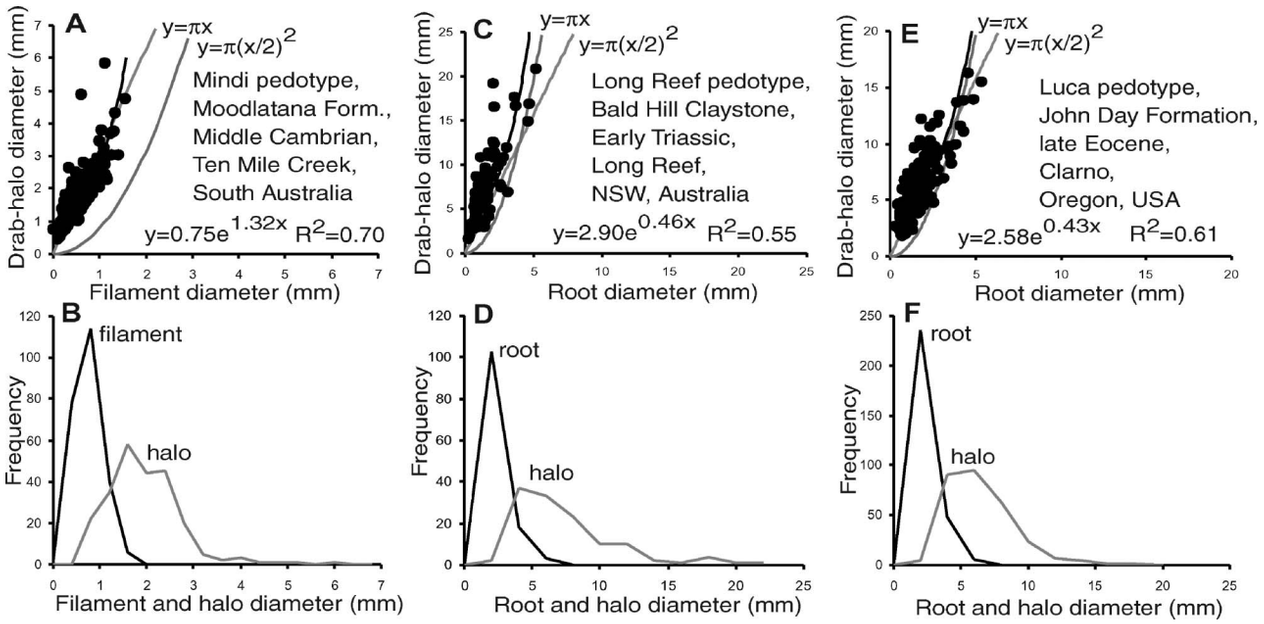

Figure 15 Root or filament diameters compared with halo diameters (a, c, e) and size distribution (b, d, f) of Cambrian drab-haloed filaments (a, b), compared with drab-haloed root traces in red paleosols of (c, d) Early Triassic (Retallack 1997b) and (e, f) Late Eocene age (Retallack *et al.* 2000).

The distinction between transparent wrinkled texture and non-transparent carpet and elephant skin texture has been made by Noffke *et al*. (2001, 2002) as class A and B microbially-induced sedimentary structures, respectively, who figured possible soil crusts from the Lower Ordovician (475 Ma, Arenigian) sandstones of Montagne

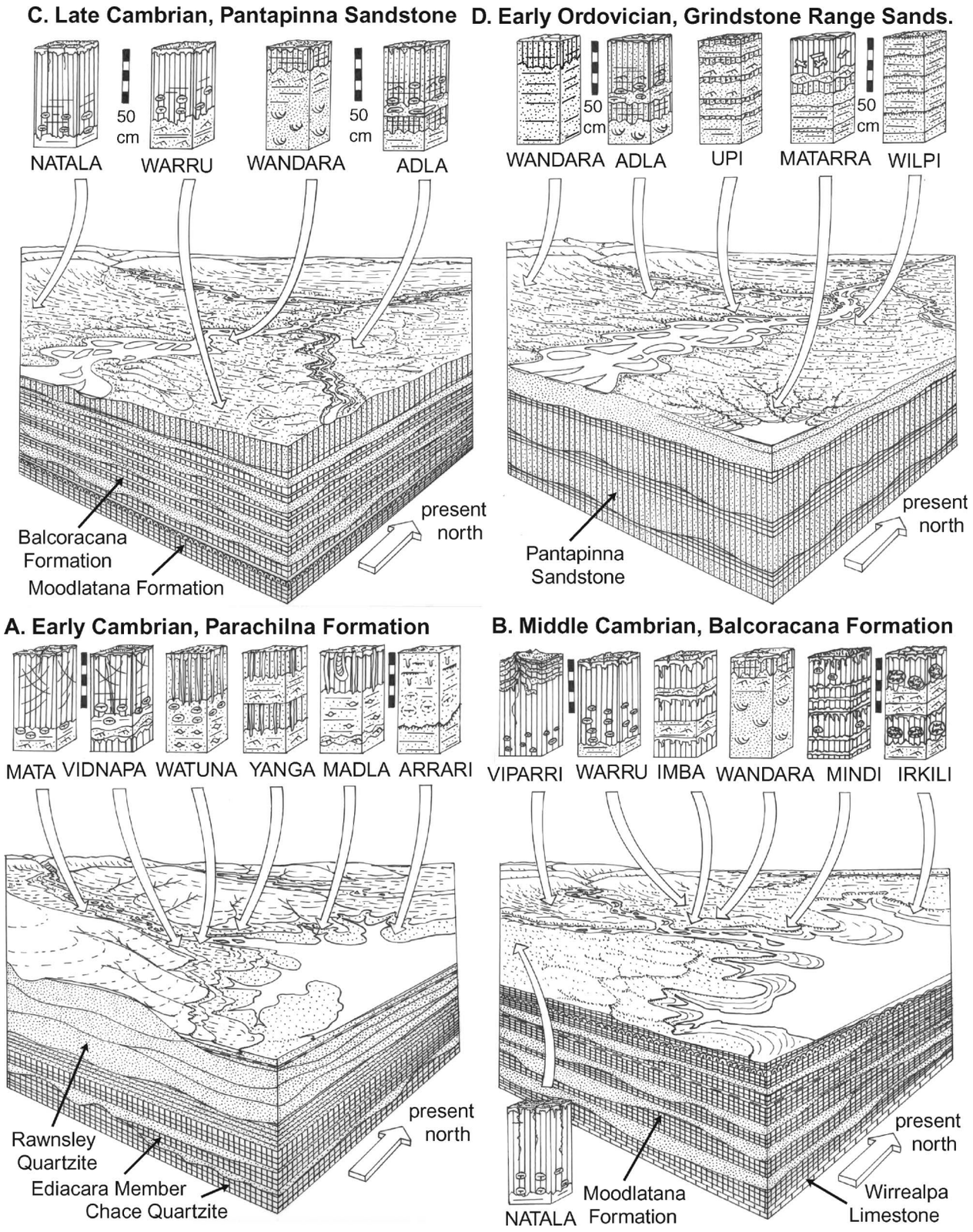

Figure 16 Reconstructed Cambrian soilscapes of South Australia.

Noire, France, and from the uppermost Neoproterozoic (550 Ma) Nudaus Formation of Namibia. Large-scale pustules 4 mm diameter and extending through 12 mm of sandstone have been figured from the Cambrian, Boxing Bay Formation of Kangaroo Island, South Australia (Madigan 1928; Daily *et al*. 1980). 'Old elephant skin texture' is also known from the uppermost Neoproterozoic (550 Ma) Ediacara Member of the Rawnsley Quartzite, South Australia (Gehling *et al*. 2005) and carpet texture from the Mesoproterozoic (1.0–1.2 Ga) Diabag Formation of northwest Scotland (Prave 2002). Such microbial cover of quartz sand was also postulated by Dott (2003) to explain the remarkable textural and chemical maturity of many Neoproterozoic and Cambrian sandstones.

Also found in presumed fluvial to playa margin paleosols (Upi) of the lower Grindstone Range Sandstone are shallow burrows comparable with *Thalassinoides* (Figure 14d). Some of the burrows are filled with red eolian silty clay, unusual at this stratigraphic level, but others are lined with red silty clay and cored by fine sandstone (Figure 14e). Upi paleosols are grey in color, with oxidised clay only at the surface and filling burrows, as in soil waterlogged by high water-table (Retallack 2001), so the burrowing organisms were probably aquatic rather than terrestrial. The burrowers also may have been marine considering conodont evidence for likely coeval marine trangression at the Cambrian–Ordovician boundary in the nearby Warburton Basin of South Australia (Jago *et al*. 2006).

Evidence for Cambrian and Ordovician life on land and in lakes is no longer surprising (Retallack 2000, 2004). Cambrian land plants have been proposed to account for organic-walled cryptospores from Middle Cambrian shales of Arizona and Kentucky (Strother 2000). Well-preserved phosphatised filaments in Middle Cambrian phosphorites of western Queensland may represent cyanobacterial colonisation of subaerially exposed phosphorite (Southgate 1986). Queensland phosphorites have also yielded large (5 mm wide) striated and branching structures interpreted as algae or lichens (Fleming & Rigby 1972: Retallack 1994). Early Ordovician (Arenigian–Llanvirnian) arthropods and liverwort-like remains from Tennessee may have lived in freshwater coastal cenotes like those of modern Yucatan (Caster & Brooks 1956; Gray 1988; Retallack 2000). Subaerial trackways from Ontario record arthropod excursions onto land in the Late Cambrian or Early Ordovician (MacNaughton *et al*. 2002). Such evidence for Cambrian non-marine life is also unsurprising from the perspective of evidence for life in Precambrian paleosols, such as supposed fossil fungi (*Witwateromyces*) and lichens (*Thucomyces*) in the Archean (2.9 Ga) carbon leader, a Fluvent paleosol of streamsides in the Witwatersrand Group of South Africa (Hallbauer & Van Warmelo 1974; Hallbauer *et al*. 1977; MacRae 1999; age from de Wit *et al*. 1992). The carbon is biogenic considering its light isotopic composition (–22 to –27‰ $\delta^{13}C$), presence of pristane and phytane, and pentose/hexose ratio of unity (Prashnowsky & Schidlowski 1967). Some of the *Thucomyces* tubes have been considered artefacts of acid preparation (Cloud 1976), but this cannot explain specimens in thin-section cut by metamorphic veins (MacRae 1999). The view that these are hydrocarbon spindles created during hydrothermal fluid migration (Barnicoat *et al*. 1997) is difficult to reconcile with intimately associated kaolinite also found in underlying paleosols (Frimmel & Minter 2002). Fragments of lichens have also been found in the Neoproterozoic (0.6 Ga) Doushantou Formation of China (Yuan *et al*. 2005). Microspheroidal forms in laminated chert in a paleosol have been reported with the unusual carbon isotopic composition of –40‰ $\delta^{13}C$, indicative of methanogenic microbes, in the 2.7 Ga Mt Roe paleosol of Western Australia (Rye & Holland 2000). Unusually high carbon isotopic values (–16 to –14‰ $\delta^{13}C$) in a 2.6 Ga paleosol near Schagen, South Africa, may indicate hypersaline microbial communities (Watanabe *et al*. 2000). Thus, some diversity of microbial life is apparent in Precambrian paleosols (Retallack 2001).

CONCLUSIONS

Evidence of paleosols can now be used to visualise Cambrian landscapes (Figure 16). Cambrian paleosols included Rudosols, Hydrosols, Tenosols, Calcarosols and Dermosols (Table 1), in soilscapes similar to those of the Flinders Ranges and surrounding regions today (Wells 1996). In the Food and Agriculture Organization (FAO 1978) map of Australian soils, the soilscape of the Parachilna Formation is like that now around Spencer Gulf, South Australia (map unit Xk40–1/2b). Billy Creek to Balcoracana Formation soilscapes were comparable with those around Lake Callabonna (map unit Vc52–3a), Pantapinna Sandstone soilscapes like floodplains of Wattiwarriganna Creek southeast of Coober Pedy (map unit Xb38–2b), all in South Australia, and Grindstone Range Sandstone soilscapes like the basin of Lake Amadeus, Northern Territory (map unit Zo36–2a). These are surprisingly continental soilscapes for Cambrian landscapes prone to occasional marine transgression (Jago *et al*. 2002, 2006), but inland South Australian lakes have not always been so remote from the sea, as indicated by their Oligocene–Miocene (25–20 Ma) foraminifera and dolphins (Fordyce 1983; Woodburne *et al*. 1993). Exhumed Cambrian fluvial landscapes in the Northern Territory suggested to Stewart *et al*. (1986) that Cambrian landscapes were very similar to modern landscapes. None of the paleosols show the highly acidic and deep weathering of Podosols, Ferrosols and Kandosols (Isbell 1998), which form in wetter and warmer climates than these Cambrian paleosols (McKenzie *et al*. 2004). None of the paleosols show thick surface organic horizons of Organosols, or clay-enriched horizons of Kurosols, Sodosols and Chromosols, or human influence of Anthroposols (of Isbell 1998), predating evolution of swamp vegetation, trees and humans, respectively (Retallack 2001). Lack of such deeply weathered soil types may explain the unusual persistence of feldspar in Cambrian paleosols (Figures 5, 6) and sandstones (Basu 1981; Dott 2003). Although barren of obvious vascular land plants, many of these ancient soils may have been stabilised by thick biological soil crusts of microbes and microbial consortia such as lichens, and some coastal and lake margin soils had

aquatic or marine animals in their waterlogged subsurface horizons.

This study has developed 10 criteria for distinguishing intertidal paleosols from alluvial and playa paleosols. Some of these are obvious, but all are useful in what has proven to be a difficult distinction to make in Cambrian and Ordovician rocks. (i) Marine trace fossils such as *Diplocraterion* are found in intertidal paleosols of the Parachilna Formation (Figure 14a), though their abundance and diversity declines in paleosols with proportionally more clay skins, oxidation rinds and slickensides as evidence of well-drained soil formation; (ii) marine-influenced paleosols include marine fossils such as trilobites stranded in red shale (Pocock 1970), but fluvial and playa paleosols are unfossiliferous; (iii) marine-influenced paleosols have halite hopper casts (Figure 9a), not found in fluvial paleosols; (iv) marine-influenced paleosols are within sequences of flaser-bedded siltstones (tidalites), but fluvial paleosols are within massive red claystones associated with trough cross-bedded sandstone paleochannels (Figure 10); (v) marine-influenced paleosols contain displacive gypsum crystals, which easily pushed aside soupy sediment (Figure 11g), whereas fluvial and playa paleosols have replacive gypsum nodules that have grown within firm soil matrix (Figure 11c); (vi) marine-influenced paleosols have sparry calcite and dolomite cements (Figure 11b), whereas fluvial and playa paleosols have nodular micritic nodules of low magnesian calcite with the displacive and replacive microfabrics of soil carbonate (Figure 11f); (vii) marine-influenced paleosols have rounded, graded and well-sorted grains deposited by traction currents of waves and tides, whereas fluvial and playa paleosols have highly angular and poorly sorted silt grains as evidence of largely eolian deposition, as in loess (Figures 11a, 12); (viii) marine-influenced paleosols show prominent relict bedding pre-dating red hematite stain and other geochemical alteration, whereas fluvial paleosols show slickensides and other soil structures including the cracked-ridge deformation of Vertisols (Figure 10a, b); (ix) marine-influenced paleosols have muted geochemical variation within the profile, particularly in base depletion, and also have much reduced iron as an indication of gleisation, unlike fluvial and playa paleosols (Figures 5, 6); and (x) marine-influenced paleosols have sharp-peaked clay minerals on X-ray diffractometer traces, whereas clay peaks from fluvial and playa paleosols are broad and ill-defined as usual in complex clays of soils (Figure 8). From this perspective, red colour and oxidation has proved to be a good indicator of terrestrial facies, as in geologically younger paleosols (Retallack 2001). The Cambrian is not unique in having marine redbeds. Cambrian paleosols have shown to be limited in diversity, compared, for example with 26 pedotypes from 45–30 Ma in Oregon (Retallack *et al*. 2000), but not so different from modern soils as they could have been.

ACKNOWLEDGEMENTS

Barbara and Warren Fargher graciously allowed access to Wirrealpa Station. Permission for fieldwork was approved by the South Australian Department of Environment and Heritage and Flinders Ranges National Park. Brian Logan and Michael Willison helped with examination of Mt Frome cores at the PIRSA core facility in Glenside. Comments from two anonymous journal reviewers greatly improved the manuscript. Funded by American Chemical Society PRF grant 45257-AC8.

REFERENCES

Álvaro J. J., Van Vliet-Lanoë B., Vennin E. & Blanc-Valleron M-M. 2003. Lower Cambrian paleosols from the Cantabrian Mountains (northern Spain): a comparison with Neogene–Quaternary estuarine analogues. *Sedimentary Geology* **163**, 67–84.

Barnicoat A. C., Henderson I. H. C., Knipe R. J., Yardley B. W. D., Napier R. W., Fox N. P. C., Kenyon A. K., Muntingh D. J., Strydom D., Winkler K. S., Lawrence S. R. & Cornford C. 1997. Hydrothermal gold mineralization in the Witwatersrand Basin. *Nature* **386**, 820–824.

Basu A. 1981. Weathering before the advent of land plants: evidence from unaltered K-feldspars in Cambrian–Ordovician arenites. *Geology* **9**, 132–133.

Belknap J., Büdel B. & Lange O. L. 2000. Biological soil crusts: characteristics and distribution. *In*: Belknap J. & Lange O. L. eds. *Biological Soil Crusts: Structure, Function and Management*, pp. 3–55. Springer, Berlin.

Bengtson S., Conway-Morris S., Cooper B. J., Jell P. A. & Runnegar B. N. 1990. Early Cambrian fossils from South Australia. *Association of Australasian Paleontologists Memoir* **9**.

Brasier M. D., Anderson M. M. & Corfield R. M. 1992. Oxygen and carbon isotope stratigraphy of early Cambrian carbonates in southeastern Newfoundland and England. *Geological Magazine* **129**, 265–279.

Breuning-Madsen H. & Awadzi T. W. 2005. Harmattan dust deposition and particle size in Ghana. *Catena* **63**, 23–38.

Briden J. C. 1967. Preliminary palaeomagnetic results from the Adelaide System and Cambrian of South Australia. *Transactions of the Royal Society of South Australia* **91**, 17–25.

Brooks H. K. 1955. Clastic casts of halite crystal imprints from the Rome Formation (Cambrian) of Tennessee. *Journal of Sedimentary Petrology* **25**, 67–71.

Burtt A. C., Abbot P. J. & Fanning C. M. 2000. Definition of Teal Flat and Marne River volcanics and associated shear zone. *MESA Journal* **17**, 37–43.

Burtt A. C. & Phillips D. 2003. $^{40}Ar/^{39}Ar$ dating of muscovite from a pegmatite in Kinchina Quarry, near Murray Bridge. *MESA Journal* **28**, 50–52.

Calver C. R. 2000. Isotope stratigraphy of the Ediacarian (Neoproterozoic III) of the Adelaide Rift Complex, Australia, and the overprint of water column stratification. *Precambrian Research* **100**, 121–150.

Caster K. E. & Brooks H. K. 1956. New fossils from the Canadian–Chazyan (Ordovician) hiatus in Tennessee. *Bulletins of American Paleontology* **36**, 157–199.

Chen Y. 1994. Laterite in Yuanmou Basin of Yunnan, China. *Haiyang Dizhi yu Disiji Dizhi (Marine Geology and Quaternary Geology)* **14**, 75–86.

Chen Y. D. & Liu S. F. 1996. Precise U–Pb zircon dating of a post-D_2 meta-dolerite; constraints for rapid tectonic development of the southern Adelaide fold belt during the Cambrian. *Journal of the Geological Society of London* **153**, 83–90.

Clarke J. D. A. 1990. An Early Cambrian carbonate platform near Wilkawillina Gorge, South Australia. *Australian Journal of Earth Sciences* **37**, 471–483.

Cloud P. E. 1976. The beginnings of biospheric evolution and their biogeochemical consequences. *Paleobiology* **2**, 352–387.

Compston W., Crawford A. R. & Bofinger V. M. 1966. A radiometric estimate of the duration of sedimentation in the Adelaide Geosyncline, South Australia. *Journal of the Geological Society of Australia* **13**, 229–276.

Cooper J. A., Jenkins R. J. F., Compston W. & Williams I. S. 1992. Ion-probe dating of a mid-Early Cambrian tuff in South Australia. *Journal of the Geological Society of London* **149**, 185–192.

Daily B. 1976. The Cambrian of the Flinders Ranges. *In*: Thomson B. P., Daily B., Coats R. P. & Forbes B. G. eds. *Late Precambrian and Cambrian geology of the Adelaide 'Geosyncline' and Stuart Shelf, South Australia*, pp. 15–19. 25th International Geological Congress Excursion Guide **33A**.

Daily B. & Forbes B. G. 1969. Notes on the Proterozoic and Cambrian, southern and central Flinders Ranges. *In*: Daily B. ed. *Geological Excursions Handbook*, pp. 23–30. 41st ANZAAS Congress, Section 3, Adelaide.

Daily B., Moore P. S. & Rust B. R. 1980. Terrestrial–marine transition in the Cambrian rocks of Kangaroo Island, South Australia. *Sedimentology* **27**, 379–399.

Dalgarno C. R. 1964. Lower Cambrian stratigraphy of the Flinders Ranges. *Transactions of the Royal Society of South Australia* **88**, 129–144.

Dalgarno C. R. & Johnson J. E. 1966. *Parachilna Map Sheet, Geological Atlas 1:250 000 Series, Sheet SH54–13.* Geological Survey of South Australia, Adelaide.

Dalrymple G. B. 1979. Critical tables for conversion of K–Ar ages from old to new constants. *Geology* **7**, 885–560.

De Wit M. J, Ronde C. E. J., Tredoux M., Roering C., Hart R. J., Armstrong R. A., Green R. W. E., Peberdy E. & Hart R. A. 1992. Formation of an Archaean continent. *Nature* **357**, 553–561.

Diessel C. F. K. 1992. *Coal-bearing Depositional Systems.* Springer, Berlin.

Dott R. H. 2003. Importance of eolian abrasion in supermature quartz sandstone and the paradox of weathering in vegetation-free landscapes. *Journal of Geology* **111**, 387–405.

Driese S. G. & Foreman J. L. 1991. Traces and related chemical changes in a Late Ordovician paleosol, *Glossifungites* ichnofacies, southern Appalachians, USA. *Ichnos* **1**, 207–219.

Driese S. G. & Foreman J. L. 1992. Paleopedology and paleoclimatic implications of Late Ordovician vertic paleosols southern Appalachians. *Journal of Sedimentary Petrology* **62**, 71–83.

Driese S. G., Mora C. I. & Elick J. M. 1997. Morphology and taphonomy of root and stump casts of the earliest trees (Middle to Late Devonian), Pennsylvania and New York. *Palaios* **12**, 524–537.

Driese S. G., Mora C. I. & Elick J. M. 2000. The paleosol record of increasing plant diversity and depth of rooting and changes in atmospheric pCO_2 in the Siluro-Devonian. *In*: Gastaldo R. A. & DiMichele W. A. eds. *Phanerozoic Terrestrial Ecosystems*, pp. 47–61. Paleontological Society Special Paper **6**.

Driese S. G., Simpson E. & Erikson K. A. 1995. Redoximorphic paleosols in alluvial and lacustrine deposits, 1.8 Ga Lochness Formation, Mt Isa: pedogenic processes and implications for paleoclimate. *Journal of Sedimentary Research* **A66**, 58–70.

Dutch R. A., Hand M. & Clark C. 2005. Cambrian reworking of the southern Australian Proterozoic Curnamona Province: constraints from regional shear-zone systems. *Journal of the Geological Society of London* **162**, 763–775.

Eberl D. D., Srodon J., Kralik M., Taylor B. E. & Peterman Z. E. 1990. Ostwald ripening of clays and metamorphic minerals. *Science* **248**, 474–477.

Elburg M. A., Bons P. D., Foden J. & Brugger J. 2003. A newly defined Late Ordovician magmatic–thermal event in the Mt. Painter Province, northern Flinders Ranges, South Australia. *Australian Journal of Earth Sciences* **50**, 611–631.

Fike D. A., Grotzinger J. P. & Summons R. E. 2006. Oxidation of the Ediacaran ocean. *Nature* **444**, 744–747.

Firman J. B. 1994. Paleosols in laterite and silcrete profiles: evidence from the southwest margin of the Australian Precambrian Shield. *Earth-Science Reviews* **36**, 149–179.

Fleming P. J. G. & Rigby J. F. 1972. Possible land plants from the Middle Cambrian, Queensland. *Nature* **238**, 266.

Foden J., Elburg M. A., Dougherty-Page J. & Burtt A. 2006. The timing and duration of the Delamerian Orogeny; correlation with the Ross Orogen and implications for Gondwana assembly. *Journal of Geology* **114**, 189–210.

Foden J., Sandiford M., Dougherty-Page J. & Williams I. 1999. Geochemistry and geochronology of the Rathjen Gneiss: implications for the early tectonic evolution of the Delamerian Orogen. *Australian Journal of Earth Sciences* **46**, 377–389.

FAO (Food & Agriculture Organization) 1974. *Soil map of the world. Volume I. Legend.* United Nations Educational Scientific and Cultural Organization, Paris.

FAO (Food & Agriculture Organization) 1978. *Soil map of the world. Volume X, Australasia.* United Nations Educational Scientific and Cultural Organization, Paris.

Fordyce R. E. 1983 Rhabdosteid dolphins from the Middle Miocene, Lake Frome Area, South Australia. *Alcheringa* **7**, 27–40.

Frey M. 1987. Very low grade metamorphism of clastic sedimentary rocks. *In*: Frey M. ed. *Low Temperature Metamorphism*, pp. 9–58. Blackie, Glasgow.

Frimmel H. E. & Minter W. E. L. 2002. Recent developments concerning the geological history and genesis of the Witwatersrand gold deposits, South Africa. *In*: Goldfarb R. J. & Nielsen R. L. eds. *Integrated Methods for Discovery: Global Exploration in the Twenty-First Century*, pp. 17–45. Society of Economic Geologists Special Publication **9**.

Gehling J. G. 2000. Environmental interpretation and a sequence stratigraphic framework for the terminal Proterozoic Ediacara Member within the Rawnsley Quartzite, South Australia. *Precambrian Research* **100**, 65–95.

Gehling J. G., Droser M. L., Jensen S. R. & Runnegar B. N. 2005. Ediacaran organisms: relating form and function. *In*: Briggs D. E. G. ed. *Evolving Form and Function*, pp. 43–56. Yale Peabody Museum, New Haven.

Geyer G., & Shergold J. 2000. The quest for internationally recognized divisions of Cambrian time. *Episodes* **23**, 188–195.

Gibson H. J. & Stüwe K. 2000. Multiphase cooling and exhumation of the southern Adelaide Fold belt: constraints from apatite fission track data. *Basin Research* **12**, 31–45.

Gile L. H., Hawley J. W. & Grossman R. B. 1980. Soils and geomorphology in the Basin and Range of southern New Mexico: Guidebook to the desert project. *New Mexico Bureau of Mines & Mineral Resources Memoir* **39**.

Gile L. H., Peterson F. F. & Grossman R. B. 1966. Morphological and genetic sequences of carbonate accumulation in desert soils. *Soil Science* **101**, 341–360.

Gradstein F. M., Ogg J. G. & Smith A. G. 2004. *A Geologic Time Scale 2004.* Cambridge University Press, Cambridge.

Gravestock D. I. 1995. Early and Middle Palaeozoic. *In*: Drexel J. F. & Priess W. V. eds. *The Geology of South Australia. Vol. 2. The Phanerozoic*, pp. 3–61. Geological Survey of South Australia Bulletin **54**.

Gravestock D. I. & Shergold J. H. 2001. Australian Early and Middle Cambrian sequence biostratigraphy with implications for species diversity and correlation. *In*: Zhuravlev A. Y. & Riding R. eds. *The Ecology of the Cambrian Radiation*, pp. 107–136. Columbia University Press, New York.

Gray J. 1988. Evolution of the freshwater ecosystem: the fossil record. *Palaeogeography Palaeoclimatology Palaeoecology* **62**, 1–214.

Hagadorn J. W. & Bottjer D. J. 1997. Wrinkle structures: microbially mediated sedimentary structures common in subtidal siliciclastic settings at the Proterozoic–Phanerozoic transition. *Geology* **25**, 1047–1050.

Haines P. W. & Flöttmann T. 1998. Delamerian orogeny and potential foreland sedimentation: a review of age and stratigraphic constraints. *Australian Journal of Earth Sciences* **45**, 559–570.

Hallbauer D. K. & Van Warmelo K. T. 1974. Fossilized plants in thucolite from Precambrian rocks of the Witwatersrand, South Africa. *Precambrian Research* **1**, 193–212.

Hallbauer D. K., Jahns H. M. & Beltmann H. A. 1977. Morphological and anatomical observations on some Precambrian plants from the Witwatersrand, South Africa. *Geologische Rundschau* **66**, 477–491.

Hasiotis S. T. & Mitchell C. E. 1993. A comparison of crayfish burrow morphologies; Triassic and Holocene fossil, paleo- and neo-ichnological evidence, and the identification of their burrow signatures. *Ichnos* **2**, 291–314

Hu X-G., Aldridge R. J., Bergström J., Siveter D., Siveter D. J. & Feng X-H. 2004. *The Cambrian fossils of Chengjiang, China.* Blackwell, Oxford.

ISBELL R. F. 1998. *The Australian Soil Classification*. CSIRO Publishing, Collingwood.

JAGO J. B., SUN X. L. & ZANG W. L. 2002. Correlation within early Palaeozoic basins of eastern South Australia. *Primary Industries and Resources South Australia Report* **2002–33**.

JAGO J. B., ZANG W. L. SUN X. L., BROCK G. A., PATERSON J. R. & SKOVSTED C. B. 2006. A review of the Cambrian biostratigraphy of South Australia. *Palaeoworld* **15**, 406–423.

JAMES N. P. & GRAVESTOCK D. I. 1990. Lower Cambrian shelf and shelf margin buildups, Flinders Ranges, South Australia. *Sedimentology* **37**, 455–480.

JELL P. A. 1983. A large bivalve arthropod from SADME Edeowie well of probable Cambrian age. *Transactions of the Royal Society of South Australia* **107**, 123–125.

JENKINS R. J. F., COOPER J. A. & COMPSTON W. 2002. Age and biostratigraphy of Early Cambrian tuffs from SE Australia and southern China. *Journal of the Geological Society of London* **159**, 645–658.

JENSEN S., GEHLING J. G. & DROSER M. L. 1998. Ediacara-type trace fossils in Cambrian sediments. *Nature* **393**, 567–569.

KIRSCHVINK J. L. & RAUB T. D. 2003. A methane fuse for the Cambrian explosion: carbon cycles and true polar wander. *Geoscience* **335**, 65–78.

MACNAUGHTON R. B., COLE J. M., DALRYMPLE R. W., BRADDY S. J., BRIGGS D. E. B. & LUKIE T. D. 2002. First steps on land: arthropod trackways in Cambrian–Ordovician eolian sandstone, southeast Ontario. *Geology* **30**, 391–394.

MACRAE C. 1999. *Life Etched in Stone: Fossils of South Africa*. Geological Society of South Africa. Johannesburg.

MADIGAN C. T. 1928. Preliminary notes on new evidence as to the age of formations on the north coast of Kangaroo Island. *Transactions of the Royal Society of South Australia* **52**, 210–216.

MAJOR R. B. & TELUK J. A. 1967. The Kulyong Volcanics. *Geological Survey of South Australia Quarterly Geology Notes* **22**, 8–11.

MAWSON D. 1938. Cambrian and sub-Cambrian formations at Parachilna Gorge. *Transactions of the Royal Society of South Australia* **62**, 255–262.

MAWSON D. 1939a. The Cambrian sequence in the Wirrealpa Basin. *Transactions of the Royal Society of South Australia* **63**, 331–347.

MAWSON D. 1939b. The late Proterozoic sediments of South Australia. *ANZAAS Meeting Report* **24**, 79–88.

MAWSON D. & SEGNIT E. R. 1949. Purple slates of the Adelaide System. *Transactions of the Royal Society of South Australia* **72**, 276–280.

MCENTEE J. & MCKENZIE P. 1992. *Ad'ňa-mat'-ňa–English Dictionary*, M. F. Nobbs, Burnside.

MCFADDEN L. D. & TINSLEY J. C. 1985. Rate and depth of pedogenic-carbonate accumulation in soils: formulation and testing of a compartment model. *In*: Weide D. L. ed. *Soils and Quaternary Geology of the Southwestern United States*, pp. 23–41. Geological Society of America Special Paper **203**.

MCKENZIE N., JACQUIER D., ISBELL R. & BROWN K. 2004, *Australian Soils and Landscapes*. CSIRO, Melbourne.

MILNES A. R., COMPSTON W. & DAILY B. 1977. Pre-to syn-tectonic emplacement of early Palaeozoic granites in southeastern South Australia. *Journal of the Geological Society of Australia* **24**, 87–106.

MITCHELL M. M., KOHN B. P. & FOSTER D. A. 1998. Post-orogenic cooling history of eastern South Australia from apatite FT thermochronology. *In*: Van den Haute P. & de Corte F. eds. *Advances in Fission-track Geochronology*, pp. 207–224. Kluwer, Amsterdam.

MITCHELL M. M., KOHN B. P., O'SULLIVAN P. B., HARTLEY M. J. & FOSTER D. A. 2002. Low-temperature thermochronology of the Mt Painter Province, South Australia. *Australian Journal of Earth Sciences* **49**, 551–563.

MOORE P. S. 1979. Stratigraphy and depositional environments of the Billy Creek Formation (Cambrian) central and northern Flinders Ranges, South Australia. *Transactions of the Royal Society of South Australia* **103**, 197–211.

MOORE P. S. 1990. Origin of redbeds and variegated sediments, Cambrian, Adelaide Geosyncline, South Australia. *In*: Jago J. B. & Moore P. S. eds. *The Evolution of a Late Precambrian–Early Palaeozoic Rift Complex: The Adelaide Geosyncline*, pp. 334–350. Geological Society of Australia Special Publication **16**.

MOUNT J. F. 1989. Re-evaluation of unconformities separating the 'Ediacaran' and Cambrian systems, South Australia. *Palaios* **4**, 366–373.

NEMECZ E., PECSI M., HARTYANI Z. & HORVATH T. 2000. The origin of silt size grains and minerals in loess. *Quaternary International* **68/71**, 199–208.

NOFFKE N., GERDES T. & KRUMBEIN W. E. 2001. Microbially induced sedimentary structures: a new category in classification of primary sedimentary structures. *Journal of Sedimentary Research* **71**, 649–656.

NOFFKE N., KNOLL A. & GROTZINGER J. F. 2002. Sedimentary controls on the formation and preservation of microbial mats in siliciclastic deposits: a case study from the Upper Neoproterozoic of Namibia. *Palaios* **17**, 533–544.

OWEN G. 2003. Load structures: gravity-driven sediment mobilization in the shallow subsurface *In*: Van Rensbergen P., Hillis R. R., Maltman A. J. & Morley C. K. eds. *Subsurface Sediment Mobilization*, pp. 21–34. Geological Society of London Special Publication **216**.

PARKIN L. W. 1969. *Handbook of South Australian Geology*. Geological Survey of South Australia, Adelaide.

PATERSON J. R. 2005. Revision of *Discomesites* and *Estaingia* (Trilobita) from the Lower Cambrian Cymbric Vale Formation, western New South Wales: taxonomic, biostratigraphic and biogeographic implications. *Proceeding of the Linnaean Society of New South Wales* **126**, 81–93.

PATERSON J. R. & BROCK G. A. 2007. Early Cambrian trilobites from Angorichina, Flinders Ranges, South Australia, with a new assemblage from the *Pararaia bunyerooensis* zone. *Journal of Paleontology* **81**, 116–142.

PATON T. R. 1974. Origin and terminology for gilgai in Australia. *Geoderma* **11**, 221–242.

POCOCK K. J. 1970. The Emuellidae, a new family of trilobites from the lower Cambrian of South Australia. *Palaeontology* **4**, 522–562.

PRASHNOWSKY A. A. & SCHIDLOWSKI M. 1967. Investigation of a Precambrian thucolite. *Nature* **216**, 560–563.

PRAVE A. R. 2002. Life on land in the Proterozoic: evidence from the Torridonian rocks of northwest Scotland. *Geology* **30**, 811–814.

PREISS W. V. 1995. Delamerian Orogeny. *In*: Drexel J. F., Preiss W. V. & Parker A. J. eds. *The Geology of South Australia*, *Volume 1, The Precambrian*, pp. 45–60. Geological Survey of South Australia Bulletin **54**.

PRUSS S., FRAISER M., & BOTTJER D. J. 2004. Proliferation of Early Triassic wrinkle structures: implications for environmental stress following the end-Permian mass extinction. *Geology* **32**, 461–464.

RETALLACK G. J. 1976. Triassic palaeosols in the upper Narrabeen Group of New South Wales; Part I, Features of the palaeosols. *Journal of the Geological Society of Australia* **23**, 383–399.

RETALLACK G. J. 1991a. *Miocene Paleosols and Ape Habitats of Pakistan and Kenya*. Oxford University Press, New York.

RETALLACK G. J. 1991b. Untangling the effects of burial alteration and ancient soil formation. *Annual Reviews of Earth and Planetary Sciences* **19**, 193–206.

RETALLACK G. J. 1992. What to call early plant formations on land. *Palaios* **7**, 508–520.

RETALLACK G. J. 1994. Were the Ediacaran fossils lichens? *Paleobiology* **20**, 523–544.

RETALLACK G. J. 1997a. Early forest soils and their role in Devonian global change. *Science* **276**, 583–585.

RETALLACK G. J. 1997b. Palaeosols in the upper Narrabeen Group of New South Wales as evidence of Early Triassic palaeoenvironments without exact modern analogues. *Australian Journal of Earth Sciences* **44**, 185–201.

RETALLACK G. J. 2000. Ordovician life on land and early Paleozoic global change. *In*: Gastaldo R. A. & DiMichele W. A. eds. *Phanerozoic Terrestrial Ecosystems*, pp. 21–45. Paleontological Society Special Paper **6**.

RETALLACK G. J. 2001. *Soils of the Past*. Blackwell, Oxford.

RETALLACK G. J. 2004. Soils and global change in the carbon cycle over geological time. *In*: Holland H. D. & Turekian K. K. eds. *Treatise on Geochemistry*, **vol. 5,** pp. 581–605. Pergamon Press, Oxford.

RETALLACK G. J. 2005. Pedogenic carbonate proxies for amount and seasonality of precipitation in paleosols. *Geology* **33**, 333–336.

RETALLACK G. J., BESTLAND E. A. & FREMD T. J. 2000. Eocene and Oligocene paleosols and environmental change in central Oregon. *Geological Society of America Special Paper* **344**.

ROSE E. C. 2006. Non-marine aspects of the Cambrian Tonto Group of the Grand Canyon, USA, and broader implications. *Palaeoworld* **15**, 223–241.

RYE R. & HOLLAND H. D. 2000. Life associated with a 2.76 Ga ephemeral pond? Evidence from the Mount Roe #2 paleosol. *Geology* **28**, 483–486.

SALTZMAN M. R. 2005. Phosphorus, nitrogen, and the redox evolution of the Paleozoic oceans. *Geology* **33**, 573–576.

SHELDON N. D. & RETALLACK G. J. 2001. Equation for compaction of paleosols due to burial. *Geology* **29**, 247–250.

SHELDON N. D., RETALLACK G. J. & TANAKA S. 2002. Geochemical climofunctions from North American soils and applications to paleosols across the Eocene–Oligocene boundary. *Journal of Geology* **110**, 687–696.

SKEHAN J. W., WEBSTER M. M. J. & LOGUE D. F. 1987. Cambrian stratigraphy and structural geology of southern Narragansett Bay, Rhode Island. *In*: Roy D. C. ed. *Centennial Field Guide, v. 5, Northeastern Section*, pp. 195–200. Geological Society of America, Boulder.

SOIL SURVEY STAFF 2000. *Keys to Soil Taxonomy*. Pocahontas Press, Blacksburg.

SOUTHGATE P. N. 1986. Cambrian phoscrete profiles, coated grains and microbial processes in phosphogenesis, Georgina Basin, Australia. *Journal of Sedimentary Petrology* **56**, 429–441.

STACE H. C. T., HUBBLE G. D., BREWER R., NORTHCOTE K. H., SLEEMAN J. R., MULCAHY M. J. & HALLSWORTH E. G. 1968. *A Handbook of Australian Soils*. Rellim, Adelaide.

STEWART A. J., BLAKE D. H. & OLLIER C. D. 1986. Cambrian river terraces and ridgetops in central Australia: oldest persisting landforms. *Science* **233**, 758–761.

STOCK E. C. 1974. The clay mineralogy, petrology and environments of deposition of the Cambrian Lake Frome Group, Flinders Ranges, South Australia. MSc thesis, University of Adelaide, Adelaide (unpubl.).

STROTHER P. K. 2000. Cryptospores: the origin and early evolution of the terrestrial flora. *In*: Gastaldo R. A. & DiMichele W. A. eds. *Phanerozoic Terrestrial Ecosystems*, pp. 3–17. Paleontological Society Special Paper **6**.

SUN D-H., BLOEMENDAL J., REA D. K., AN Z-S., VANDENBERGHE J., LU H-Y., SU R-X. & LIU T-S. 2004. Bimodal grainsize distribution of Chinese loess and its paleoclimatic implications. *Catena* **55**, 325–340.

SURGE D. M. 1996. Geochemical and petrologic evidence for limited diagenesis in Lower Cambrian carbonates, South Australia: implications for photosynthesis and depth-related variations in primary productivity. MSc thesis, Indiana University, Bloomington (unpubl.).

SWINEFORD A. & FRYE J. C. 1951. Petrography of the Peoria Loess in Kansas. *Journal of Geology* **59**, 306–322.

TISSOT B. P. & WELTE D. H. 1984. *Petroleum Formation and Occurrence*. Springer, Berlin.

TUCKER M. D. 1991. Carbon isotopes and Cambrian–Precambrian boundary geology South Australia: ocean basin formation, seawater chemistry and organic evolution. *Terra Nova* **1**, 573–582.

TURNER P. 1979. Diagenetic origin of Cambrian marine red beds: Caerfai Bay shales, Dyfed, Wales. *Sedimentary Geology* **24**, 269–281.

TURNER S. P. 1996. Petrogenesis of the late Delamerian gabbroic complex at Black Hill, South Australia: implications for convective thinning of the lithospheric mantle. *Mineralogy and Petrology* **56**, 51–89.

TURNER S. P. & FODEN J. 1996. Magma mingling in late Delamerian A-type granites at Mannum, South Australia. *Mineralogy and Petrology* **56**, 147–169.

TURNER S. P., KELLEY S. P., VANDENBERG A. H. M., FODEN J. D., SANDIFORD M., & FLÖTTMANN T. 1996. Source of the Lachlan Fold Belt flysch linked to convective removal of lithosphere mantle and rapid exhumation of the Delamerian–Ross fold belt. *Geology* **24**, 941–944.

VETTER J. R., KODAMA K. P. & GOLDSTEIN A. 1989. Reorientation of remanent magnetism during tectonic fabric development: an example from the Waynesboro Formation, Pennsylvania, USA. *Tectonophysics* **165**, 29–39.

WAGGONER B. & HAGADORN J. W. 2005. Conical fossils from the Lower Cambrian of eastern California. *PaleoBios* **25**, 1–10.

WATANABE Y., MARTINI J. E. J. & OHMOTO H. 2000. Geochemical evidence for terrestrial ecosystems 2.6 billion years ago. *Nature* **408**, 574–578.

WELLS C. B. 1996. The patterns of soils of the Flinders Ranges. *In*: Davies M., Twidale C. R. & Tyler M. J. eds., *Natural History of the Flinders Ranges*, pp. 76–85. Royal Society of South Australia, Adelaide.

WHEELER R. L. 2002. Distinguishing seismic from nonseismic soft-sediment structures: criteria from seismic-hazard analysis. *In*: Ettensohn F. R., Rast N. & Brett C. E. ed. *Ancient Seismites*, pp. 1–11. Geological Society America Special Paper **359**.

WOPFNER H. 1970. Early Cambrian paleogeography, Frome Embayment, South Australia. *AAPG Bulletin* **54**, 2395–2409.

WOODBURNE M. O., MACFADDEN B. J., CASE J. A., SPRINGER M. S., PLEDGE N. S., POWER J. D., WOODBURNE J. M. & SPRINGER K. B. 1993. Land mammal biostratigraphy of the Etadunna Formation (Late Oligocene) of South Australia. *Journal of Vertebrate Paleontology* **13**, 483–515.

YUAN X-L., XIAO S-H. & TAYLOR T. N. 2005. Lichen-like symbiosis 600 million years ago. *Science* **308**, 1017–1020.

ZANG W-L. 2002, Sequence analysis and petroleum potential in the Arrowie Basin, South Australia. *Minerals and Energy Resources South Australia Report Book* **2002/024**.

ZHOU B. & WHITFORD D. J. 1994. Geochemistry of the Mt Wright Volcanics from the Woonominta Block, northwestern New South Wales. *Australian Journal of Earth Sciences* **41**, 331–340.

Received 23 June 2007; accepted 19 April 2008

SUPPLEMENTARY PAPER

APPENDIX 1: SUPPLEMENTARY INFORMATION ON CAMBRIAN PALEOSOLS OF SOUTH AUSTRALIA

Data Table 1 XRF chemical analyses of Cambrian paleosols (weight percent).

Data Table 2 Point count data on grainsize and minerals of Cambrian paleosols.

Data Table 3 Clay mineral crystallinity indices calculated from X-ray diffractometer traces.